

Superconducting Nanowire Single Photon Detector (SNSPD)

Hsin-Yeh Wu, Stathes Paganis

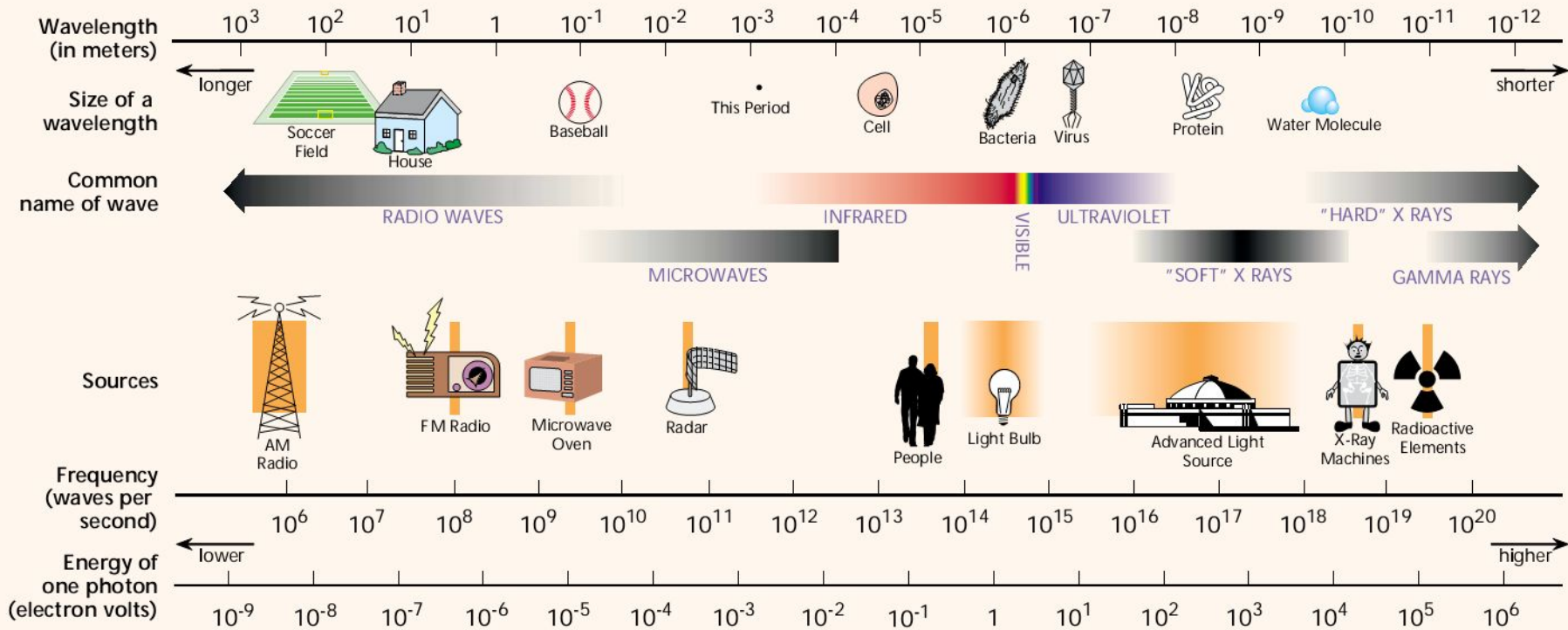
National Taiwan University

TIDC annual meeting

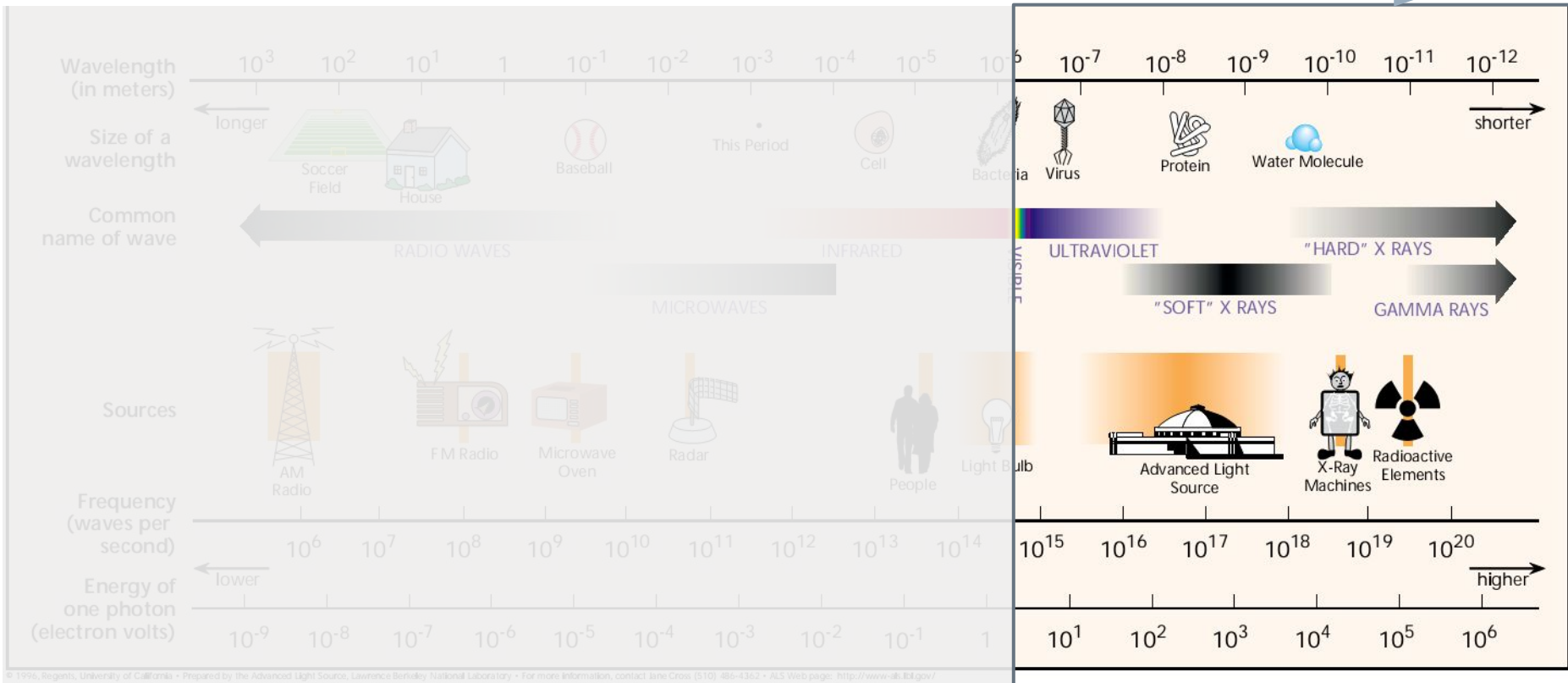
25 Nov, 2023



THE ELECTROMAGNETIC SPECTRUM



Short Wavelength, High Energy



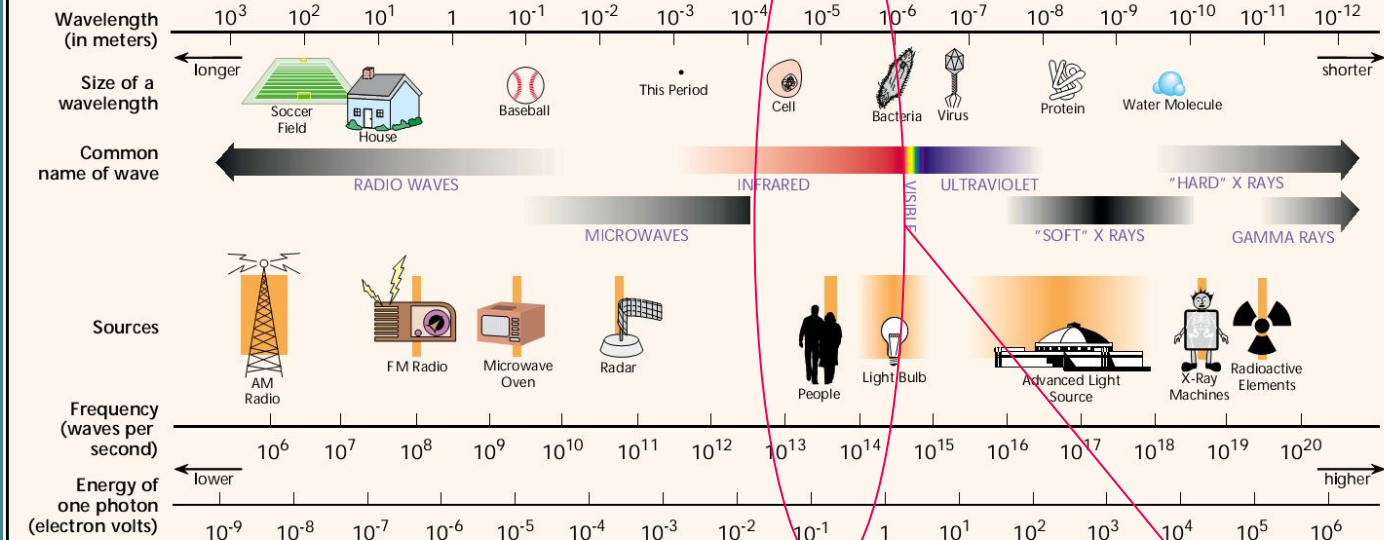
© 1996, Regents, University of California • Prepared by the Advanced Light Source, Lawrence Berkeley National Laboratory • For more information, contact Line Cross (510) 486-4362 • ALS Web page: <http://www-alk.lbl.gov/>

Rich spectrum of detectors for HEP



Source: Detector Technology Challenges – Ian Shipsey (15th Pisa meeting on Advanced Detectors)

THE ELECTROMAGNETIC SPECTRUM



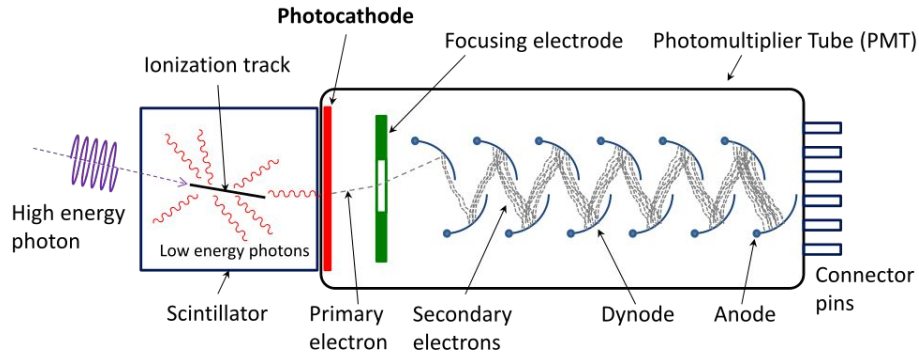
© 1996, Regents, University of California • Prepared by the Advanced Light Source, Lawrence Berkeley National Laboratory • For more information, contact Jane Cross (510) 486-4362 • ALS Web page: <http://www-rl.berkeley.edu>

Let's extend to IR Single Photon!?

Semiconductor Single Photon Detectors

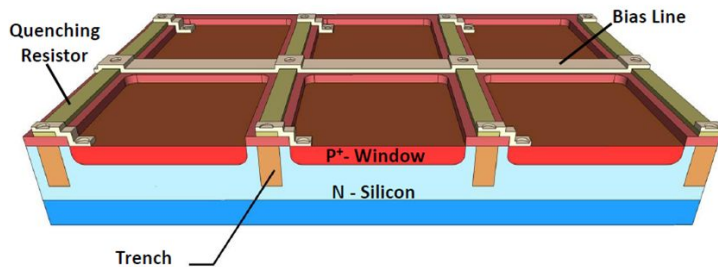
Photomultiplier Tubes (PMT)

Wikimedia Commons



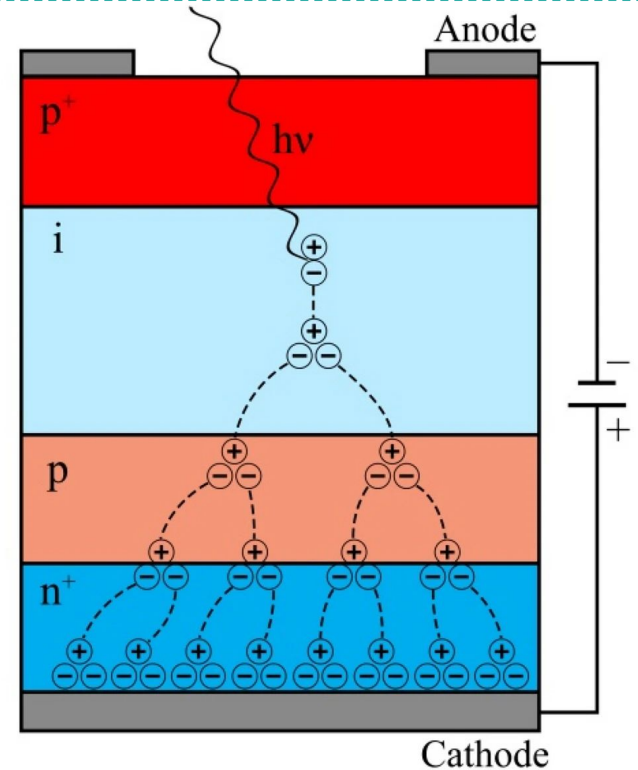
Silicon Photomultiplier (SiPM)

Section of KETEK SiPM Microcell



APPEC Communications

Single Photon Avalanche Diode (SPAD)



Izhnin, I.I., et al. Appl Nanosci 12, 253–263 (2022).

Semiconductor Single Photon Detectors

Photomultiplier Tubes (PMT)

Wikimedia Commons

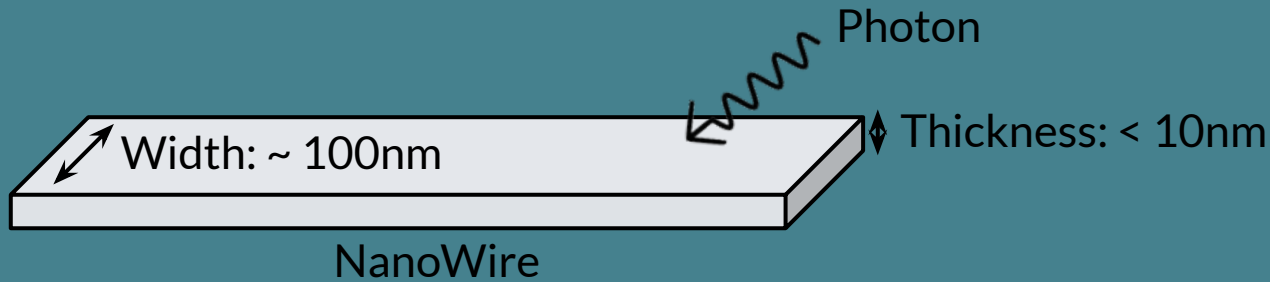
Single Photon Avalanche Diode (SPAD)

Bandgap Threshold

- Si: $\sim 1.1\text{eV}$ ($\sim 1.1\mu\text{m}$)
- Ge: $\sim 0.7\text{eV}$ ($\sim 1.7\mu\text{m}$)

Blocked impurity band solid-state photomultipliers.

- Large Dark Current



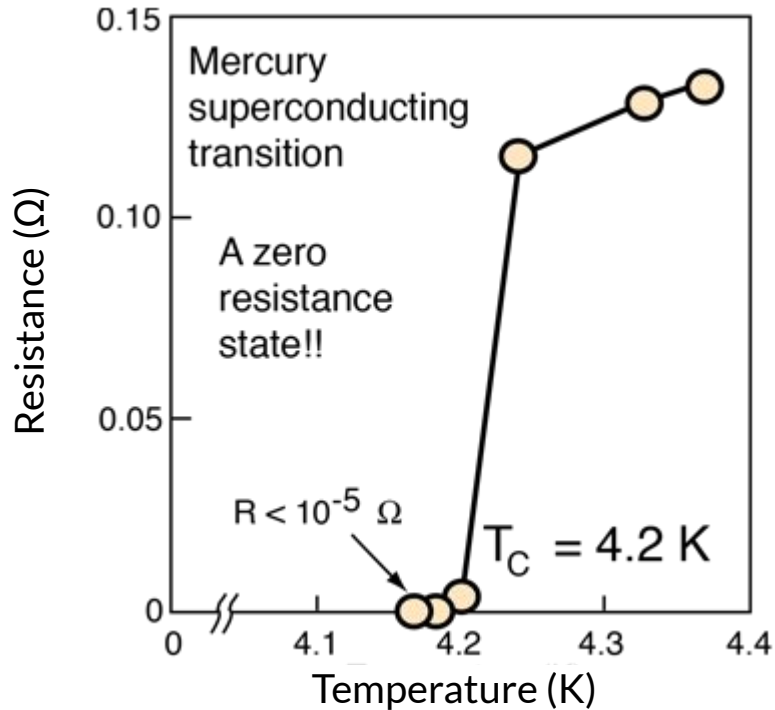
Superconductivity Nanowire Single Photon Detector (SNSPD)

Outline

- SNSPD Intro
- Fabrication and Characterization setup
- First Prototypes results
- Applications

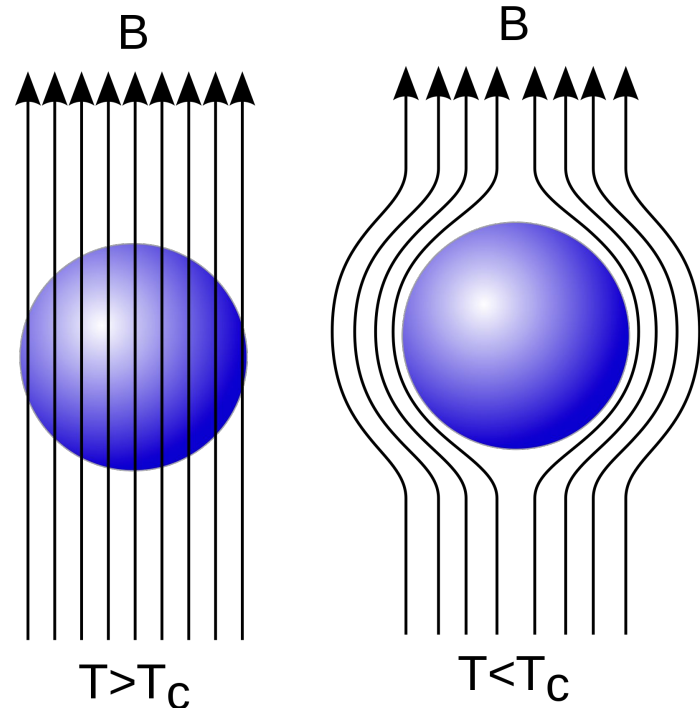
Superconductivity

Zero Resistance



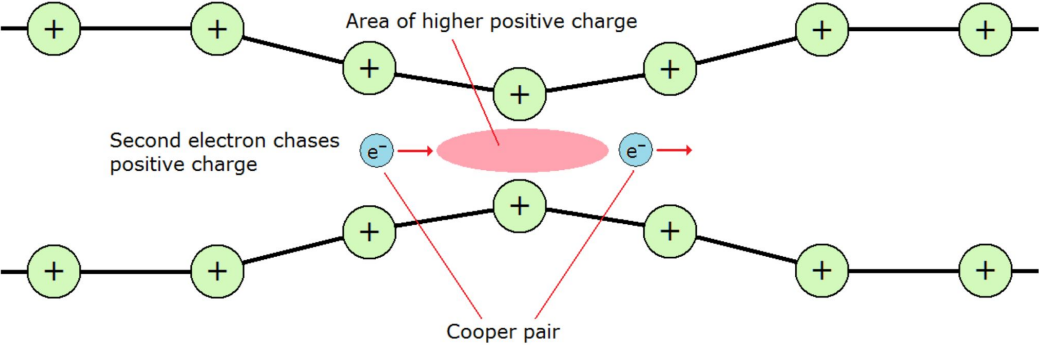
H. K. Onnes, Commun. Phys. Lab.12,120, (1911)

Meissner Effect Perfect diamagnetic (Superdiamagnetic)

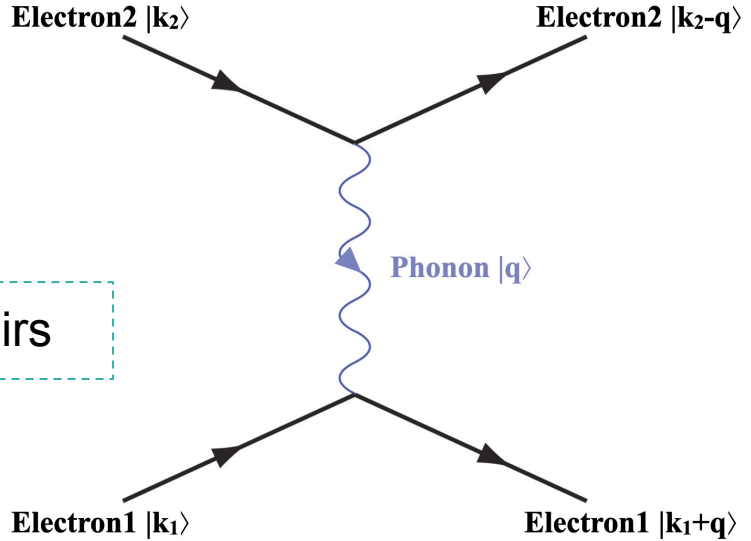


Wikimedia Commons

Cooper pairs (BCS mechanism)



$$\hat{H} \left| \vec{k}_1 \pm \vec{q} \right\rangle = \epsilon_{k_1 \pm q} \left| \vec{k}_1 \pm \vec{q} \right\rangle$$

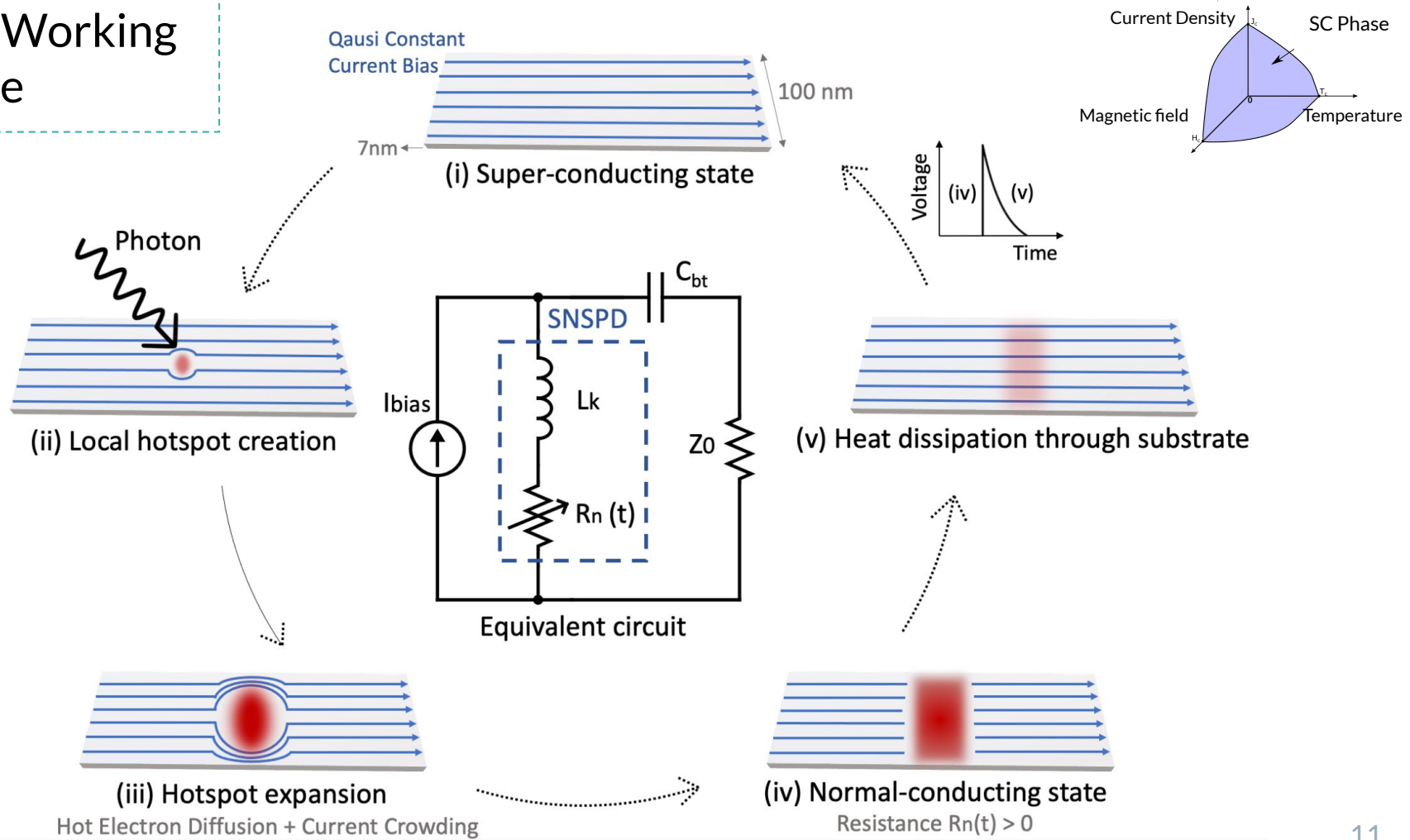


V_{e-ph-e} (Attractive) > V_{e-e} (Repulsive) \rightarrow Cooper-Pairs

- Spin-0 composite particle (boson) \rightarrow BEC Condensation
- Energy quantized \rightarrow No random scattering \rightarrow Zero Resistance
- Energy Gap Δ_{BEC} (~1meV) \rightarrow 3 orders smaller than Δ_{Si} !

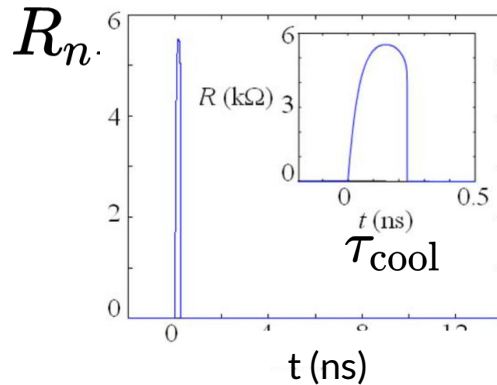
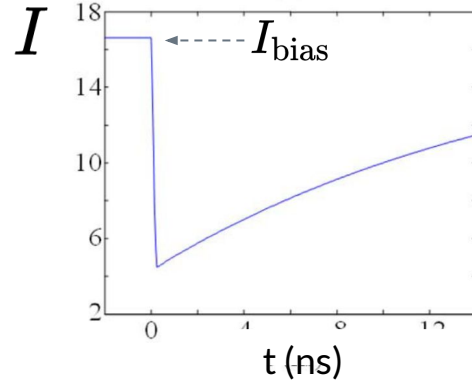
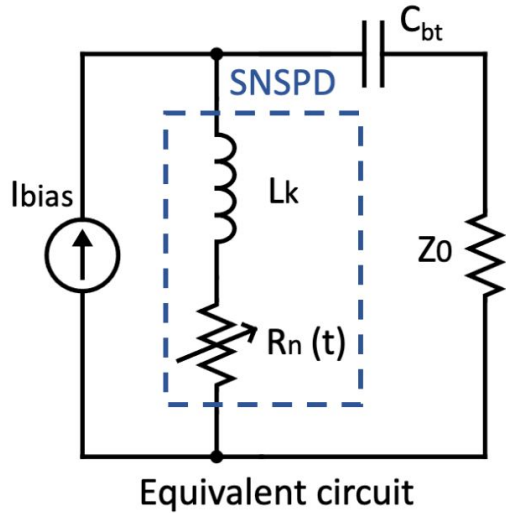
$$V = \frac{|M|^2}{(\epsilon_{\vec{k}} - \epsilon_{\vec{k}+\vec{q}})^2 - \hbar\omega_q^2}$$

SNSPD Working Principle

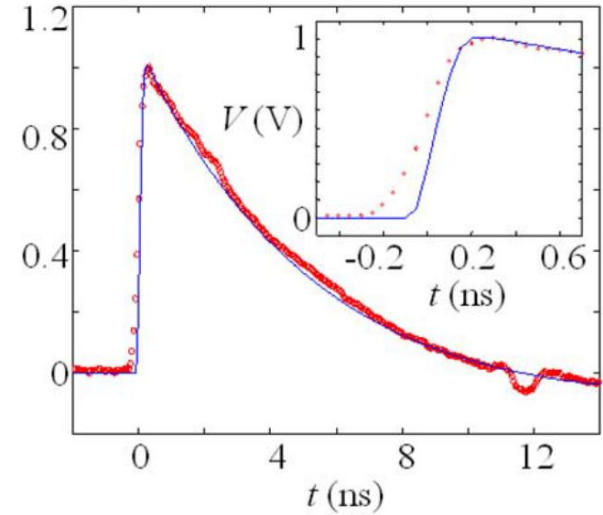


LCR Electric Circuit Model

Yang, J. K. W. et al. IEEE Transactions on Applied Superconductivity 17, 581–585 (2007)



Load (Z_0) Voltage



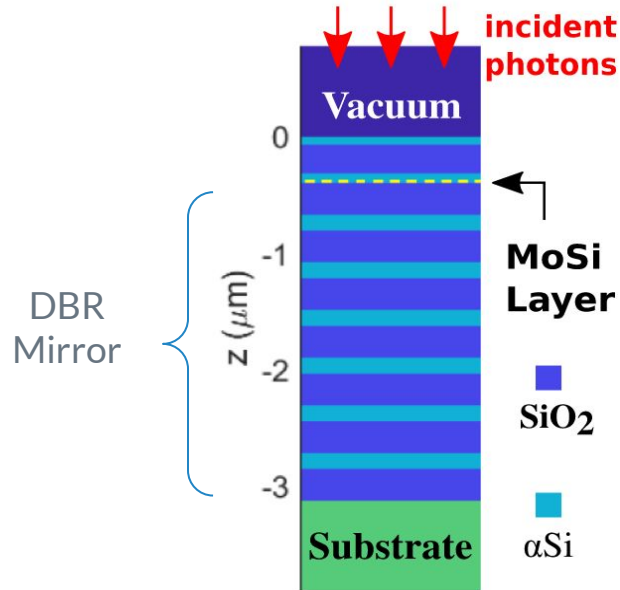
$$\tau_{\text{rise}} = \frac{L_k}{Z_0 + R_n(t)}$$

$$\tau_{\text{fall}} = \frac{L_k}{Z_0}$$

$$C_{bt} (L_k I'' + Z_0 I' + (R_n I)') = I_{\text{bias}} - I$$

State-of-the-art SNSPDs @ 1550nm

Reddy, D. V. et al. Optica 7, 1649 (2020).



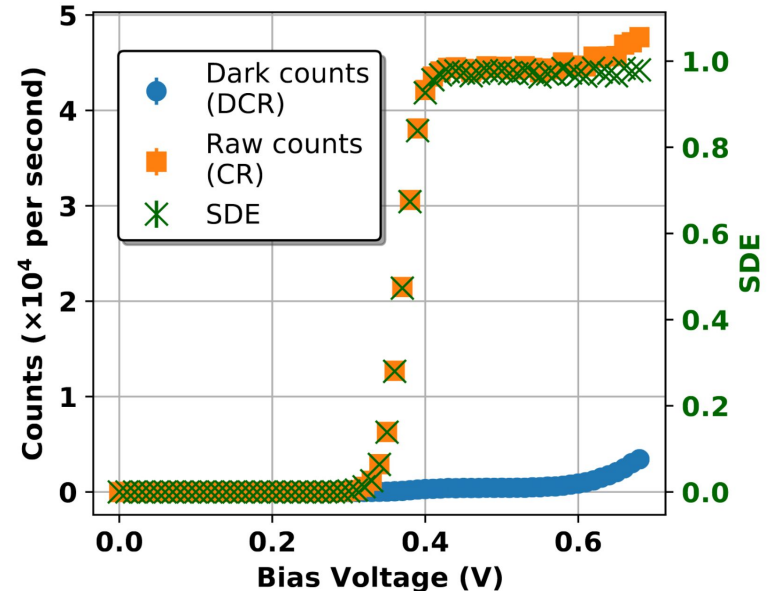
MoSi ($T_c \sim 5\text{K}$)

Width: 80nm, Pitch: 140nm

Distributed Bragg Reflector Mirror

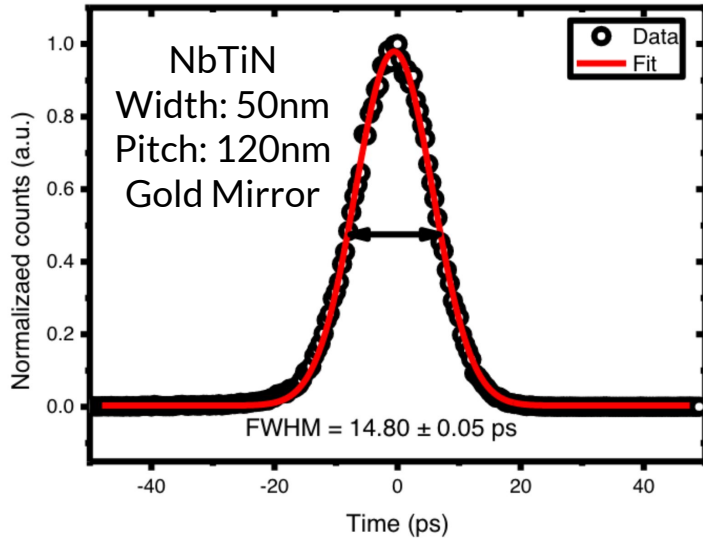
Measure Temperature $\sim 750\text{mK}$

98% System Detection Efficiency
High Count Rate
Low Dark Count Rate



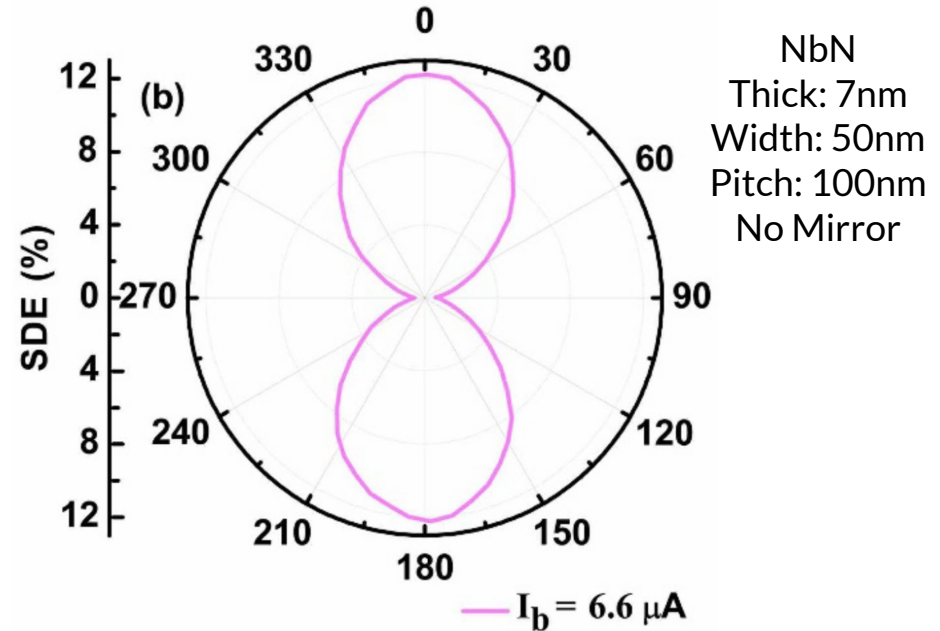
State-of-the-art SNSPDs @ 1550nm

Time Jitter < 15ps



Esmail Zadeh, I. et al. APL Photonics 2, 111301 (2017).

Polarization Sensitive



Guo, Q. et al. Sci Rep 5, 9616 (2015).

Our Roadmap

State-of-the-art

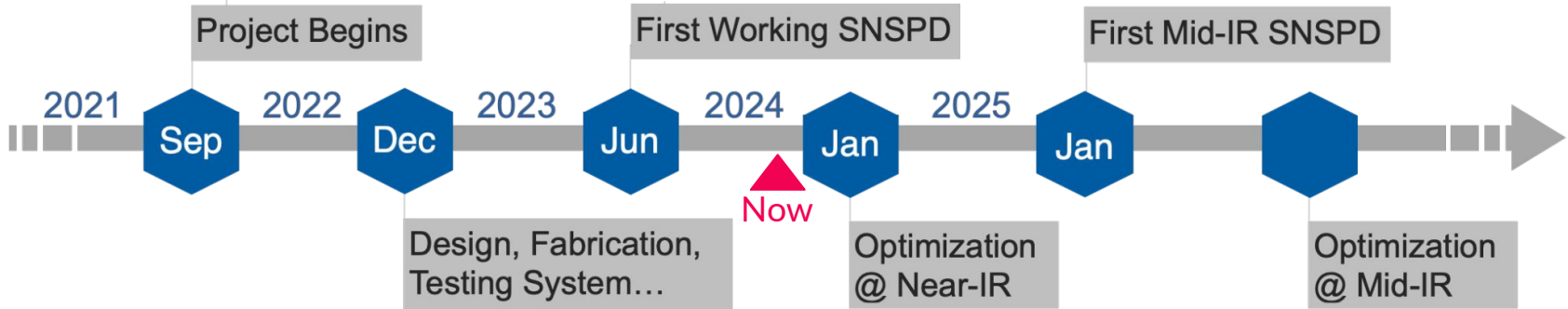
Excellent performance @ Near-IR (0.8 μ m-2 μ m)

- ~100% single photon efficiency @ 1550nm
- Low timing jitter (<15ps)
- Low Dark Count (<0.01Hz)
- Fast recovery (MHz readout rate)
- Polarization sensitive
- Multipixelized array

Goal

Extend to Mid-IR (2 μ m-20 μ m)

- All the excellent existing properties
- Broadband
- Polarization distinguishability



SNSPD Fabrication

SC Material Choice

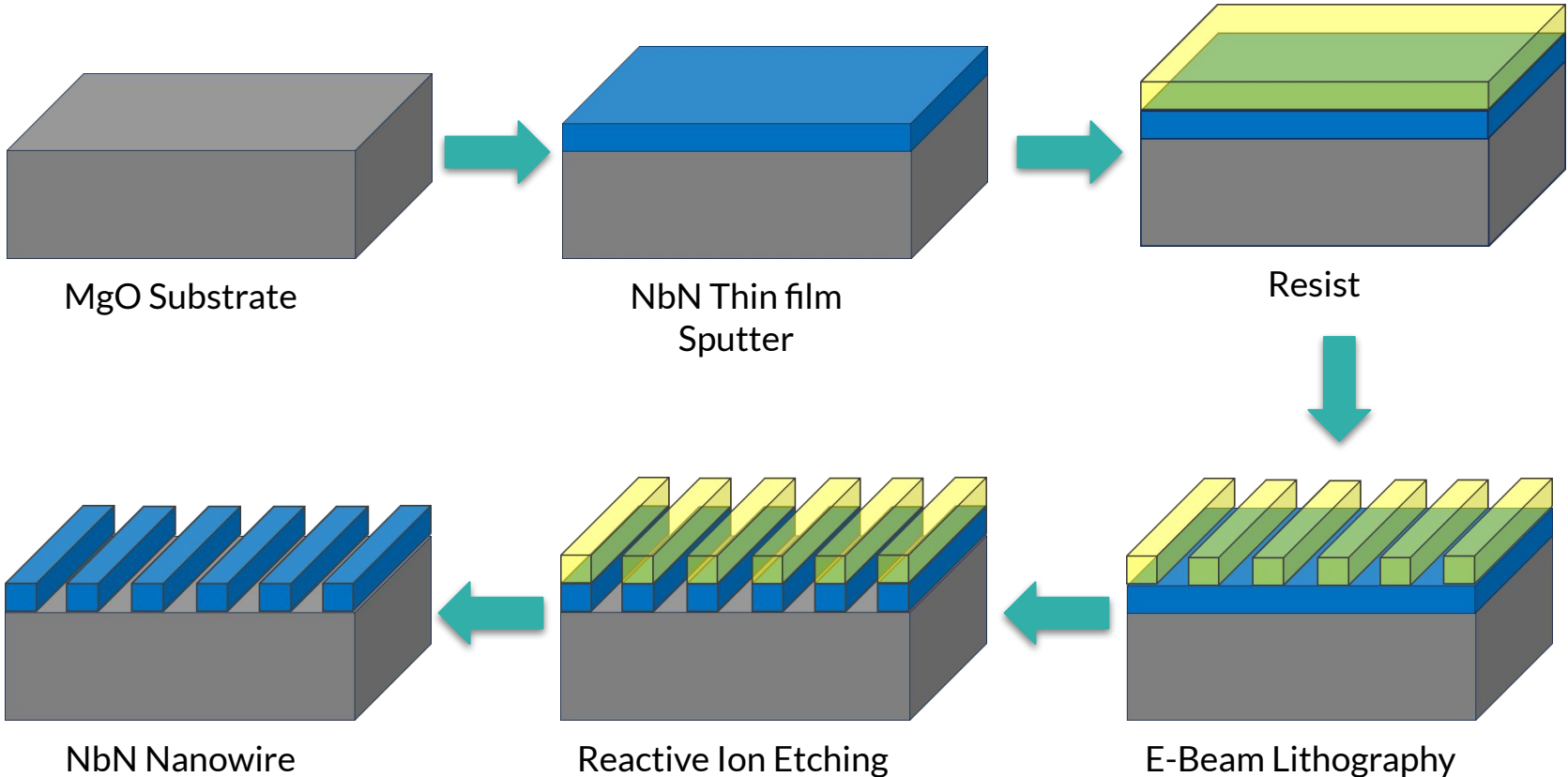
Material	T_c^* , K	$\Delta(\text{BCS})$, meV	N_{qp}^{**} (3 μm photon)
Nb	4.15	0.63	~600
✓ NbN	8.6	1.3	~300
NbTiN	9.6	1.46	~300
WSi	3.7	0.56	~700
MoSi	4.3	0.65	~600
MoGe	4.4	0.66	~600
TiN	0.4 - 4.5	0.06 – 0.68	~6000 - 600
SC-diamond	2 - 4.2	0.3 – 0.63	~1300 - 600

* Data for thin film

** Number of quasi-particles

Dmitry Morozov et. al, Proc. SPIE 10659, Advanced Photon Counting Techniques XII, 106590G (14 May 2018)

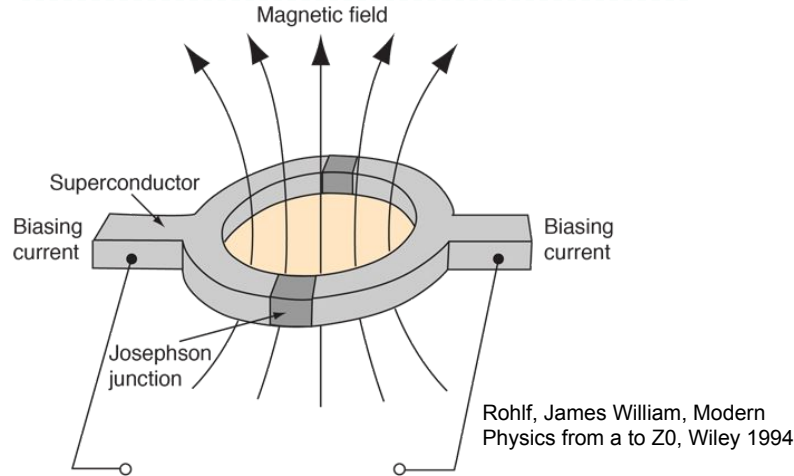
Fabrication Flow



Thin film quality characterization

Magnetic susceptibility χ_v @ 2-20K

→ Critical Temperature

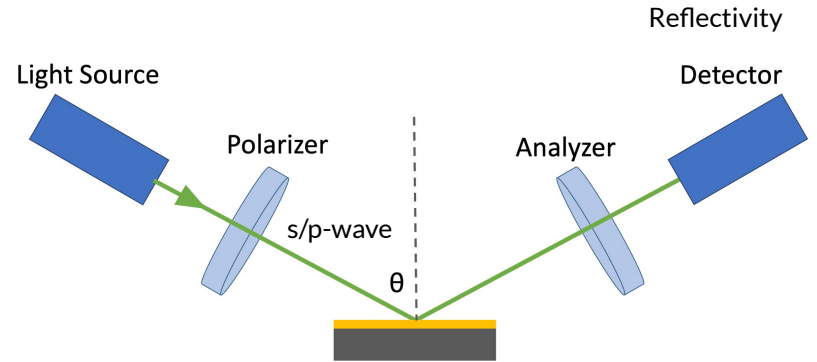


Superconducting Quantum Interference Device (SQUID)

Measured by Instrumentation Center,
Chen, I-Nan

Electric susceptibility χ_e @ 300K

→ Metallic Property



Ellipsometry

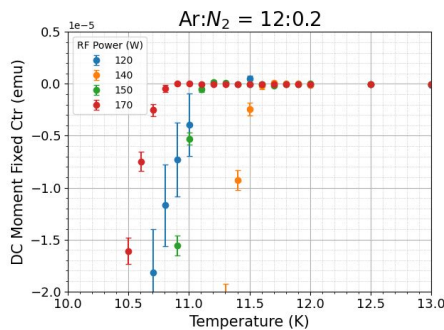
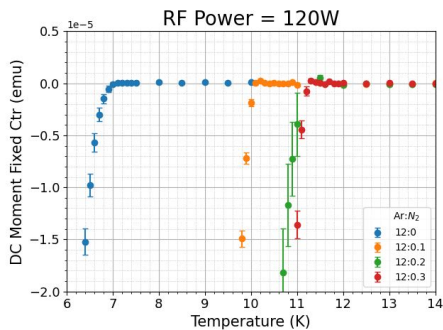
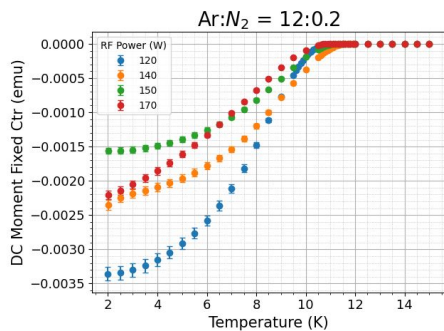
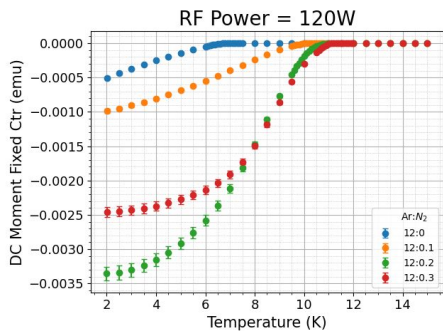
Measured by Lu's Lab,
Jing-Wei Yang


NbN Thin Film Optimization with Sputter Parameters


RF Power & Ar:N₂ Flow rate

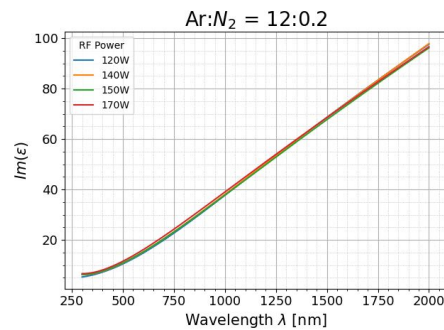
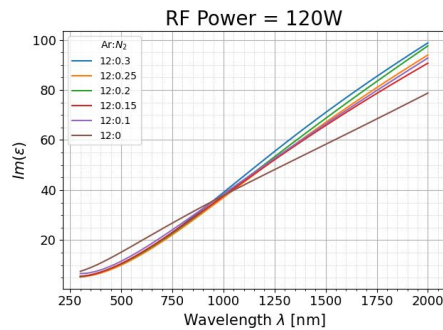
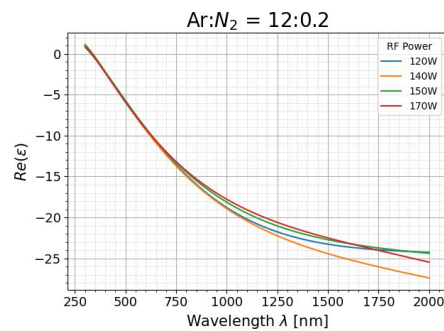
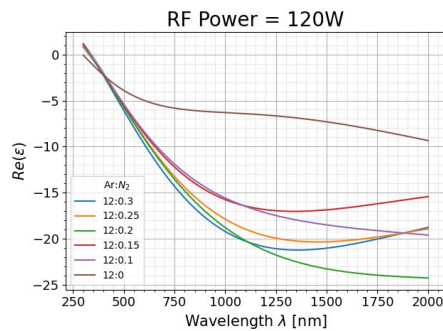
SQUID → Higher T_c (Better crystallized)


Ellipsometry → Re(ε) more negative (More metallic)
Im(ε) larger (Higher absorption)



 12:0.2 or 12:0.3

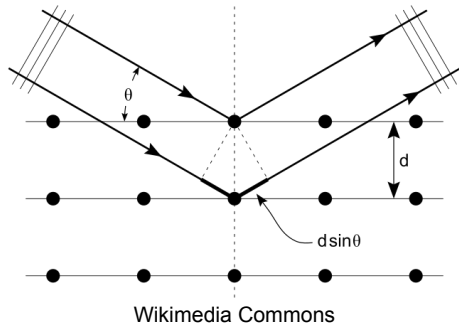
 140W



 12:0.2 or 12:0.3

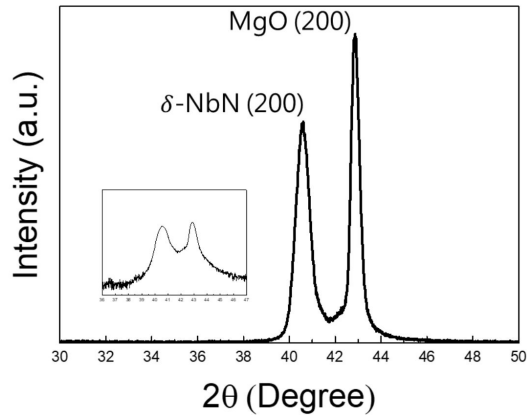
 140W

Inpurities – X-Ray Diffraction



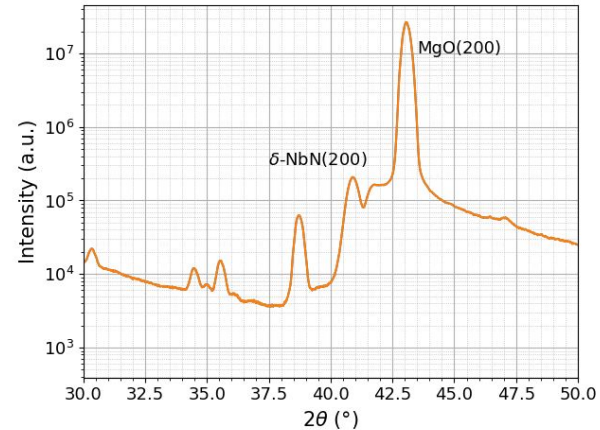
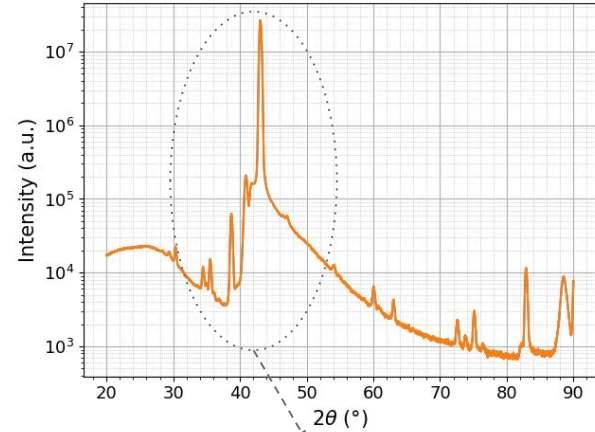
Crystal Structure

2022 Measured



Jing-Wei Yang, <https://hdl.handle.net/11296/5376n3>

2023 Measured

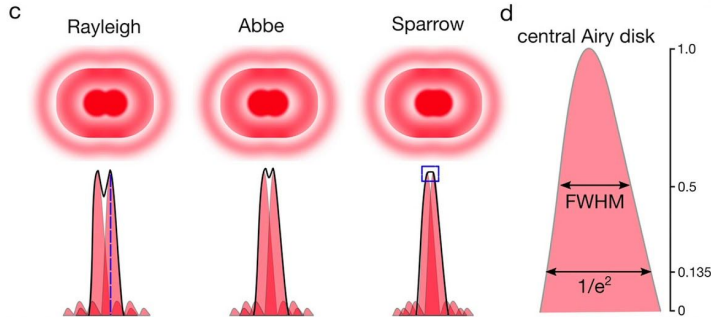


E-Beam Lithography

Abbe's Diffraction Limit

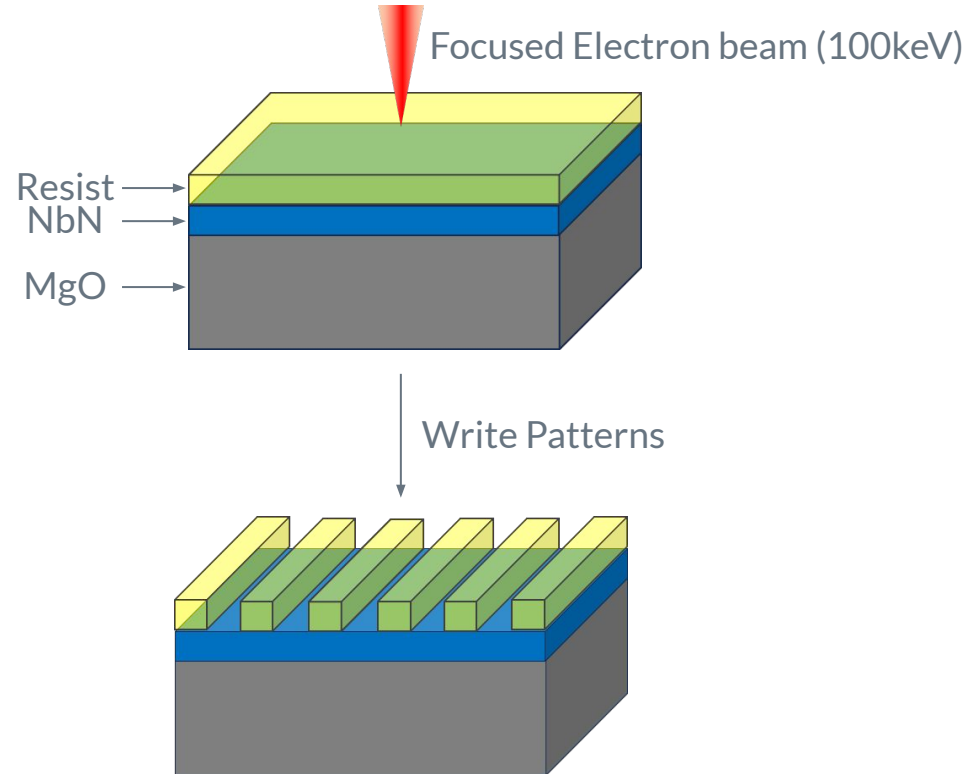
$$d = \frac{\lambda}{2NA}$$

Lithography Resolution



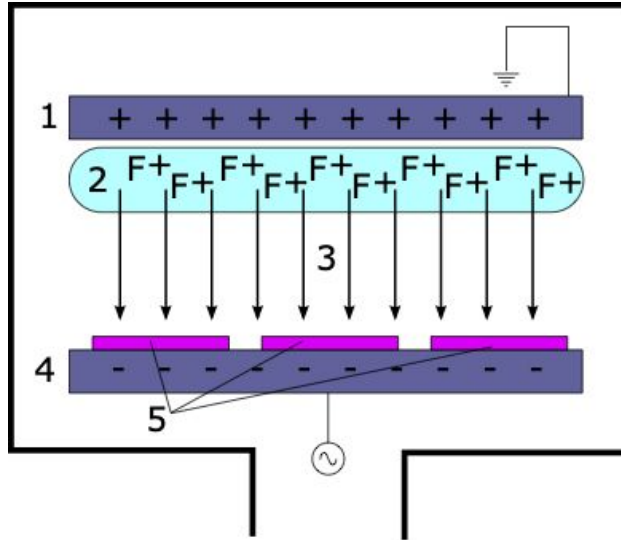
©Erdinc Sezgin, J. Phys.: Condens. Matter 29 (2017) 273001

PhotoLithography with UV(400nm) \rightarrow $d \sim 200\text{nm}$
Nanowire width: 100nm \rightarrow E-Beam Lithography



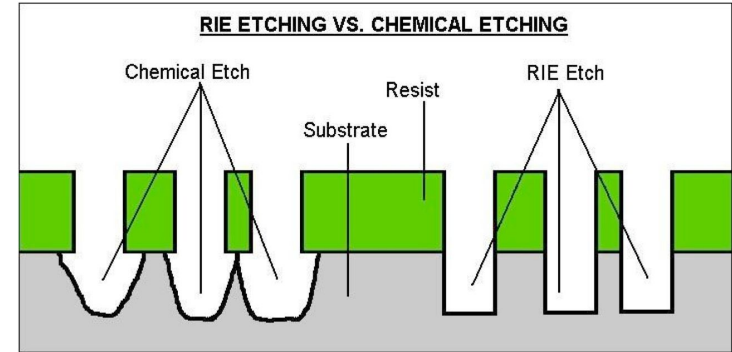
Reaction Ion Etching

RIE Principle similar to Sputter →
Ion acceleration bombardment

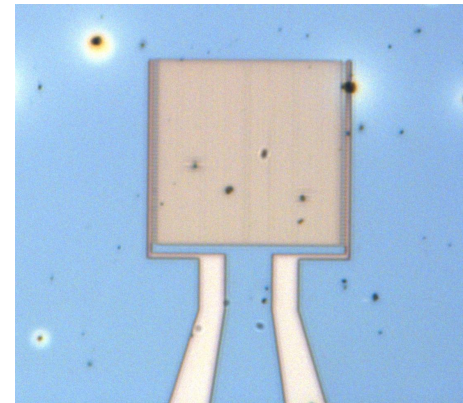


By Dollhaus, modified by Adobe1018 to show correct electric charges.
- <https://en.wikipedia.org/wiki/File:Riedigram.gif#file>, CC BY-SA 3.0,
<https://commons.wikimedia.org/w/index.php?curid=29191041>

Higher precision compared to
traditional chemical etch

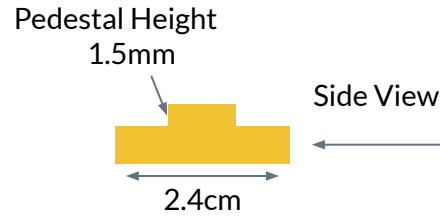
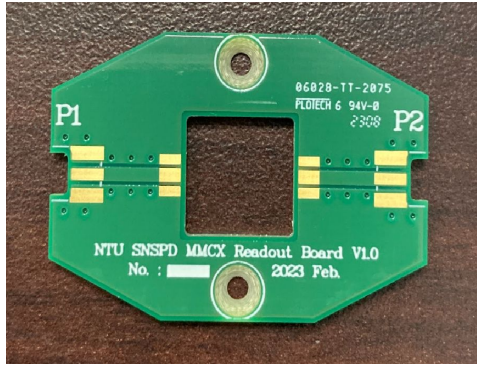


After Etching → NbN Nanowire

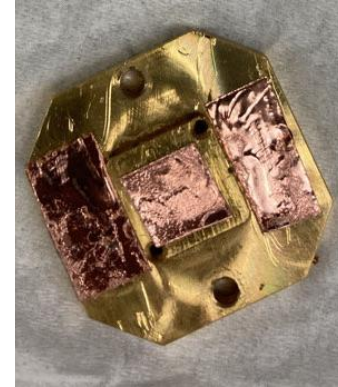


SNSPD Characterization Setup

SNSPD Device Preparation



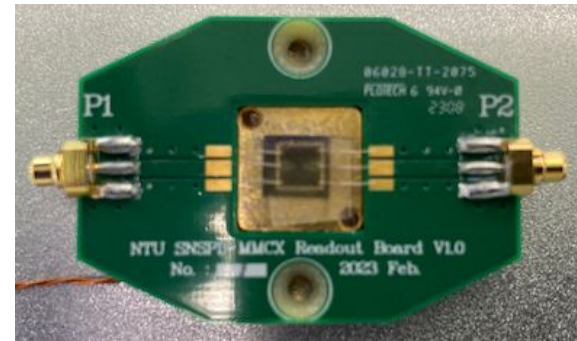
Gold-plated Mount



2 Channel SNSPD Readout PCB

Grounded Coplanar Waveguide (GCPW)
MMCX connector
Designer: Hsin-Yeh, Wu
Drawn by: Jenny Huang
Fabrication: Plotech

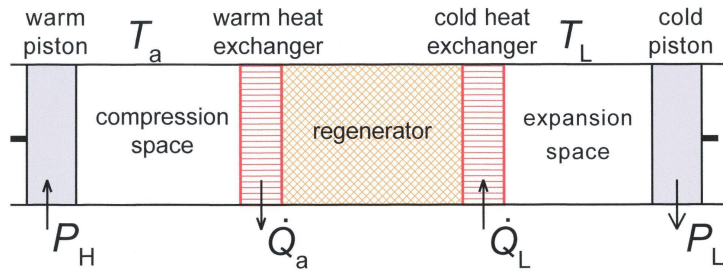
SNSPD Device



Wirebond: Ouchen

Cryogenics

Cryocooler: Stirling Refrigerator



By Adwaele - Made by SliteWrite, CC BY-SA 3.0,
<https://commons.wikimedia.org/w/index.php?curid=124814496>

attoDRY800

Pulsetube
Optical table implemented
@ Prof. Yu-Rong Lu's Lab (AS)

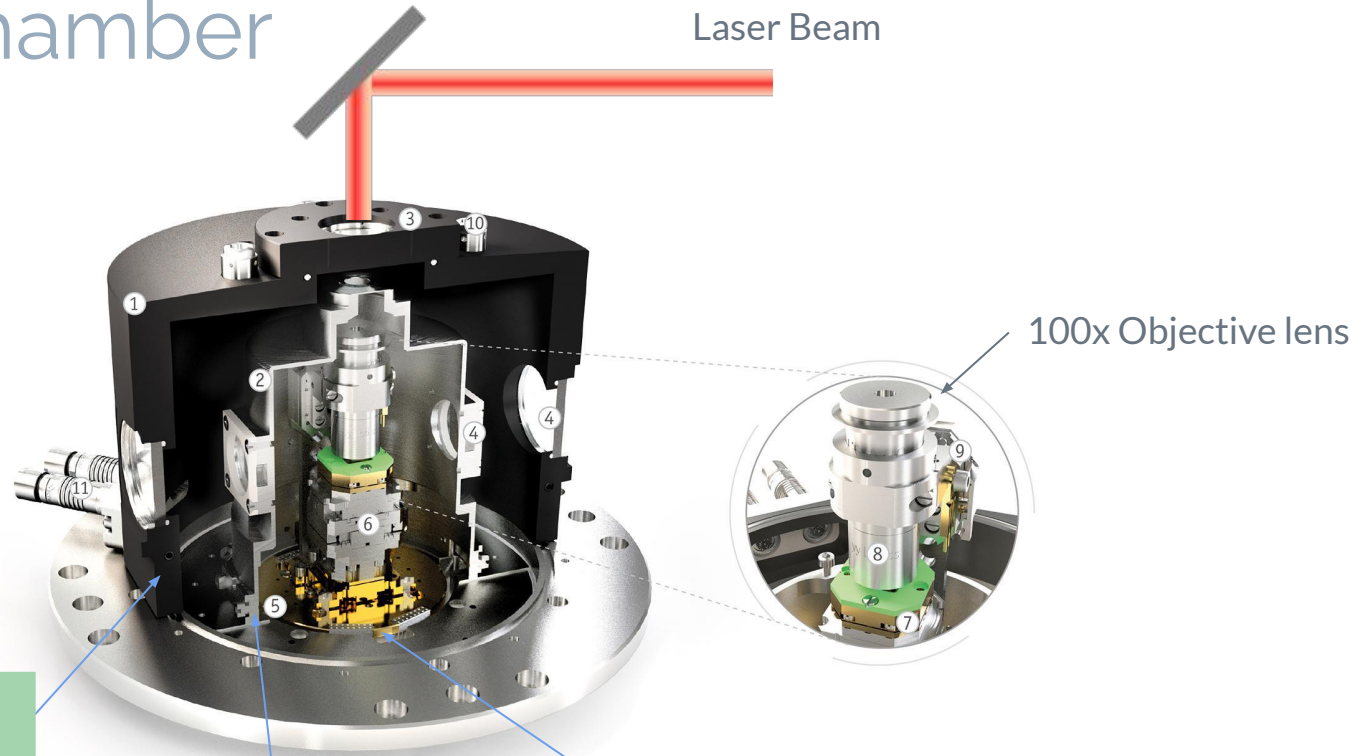


01 optical table (included)
02 cryocooler
03 cold breadboard

04 customizable vacuum shroud
05 touchscreen user interface
06 obstruction free work space

Vacuum chamber

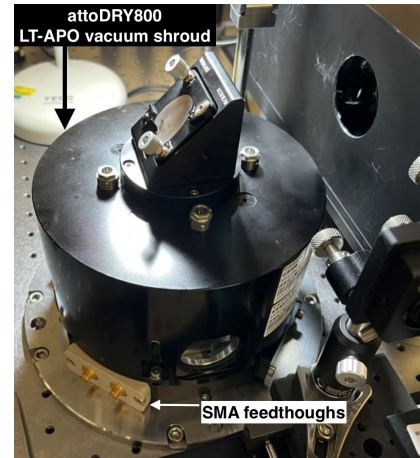
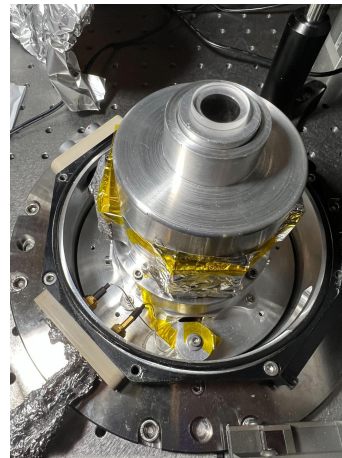
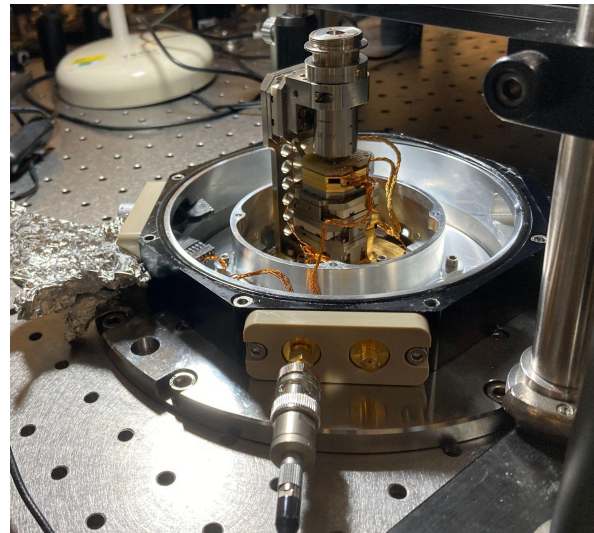
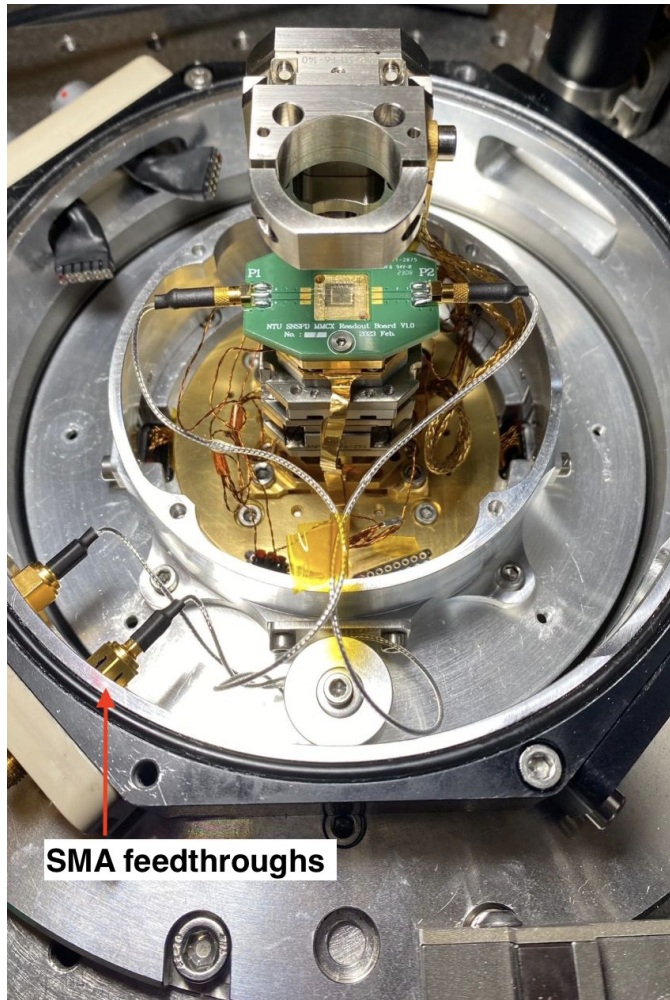
Laser Beam



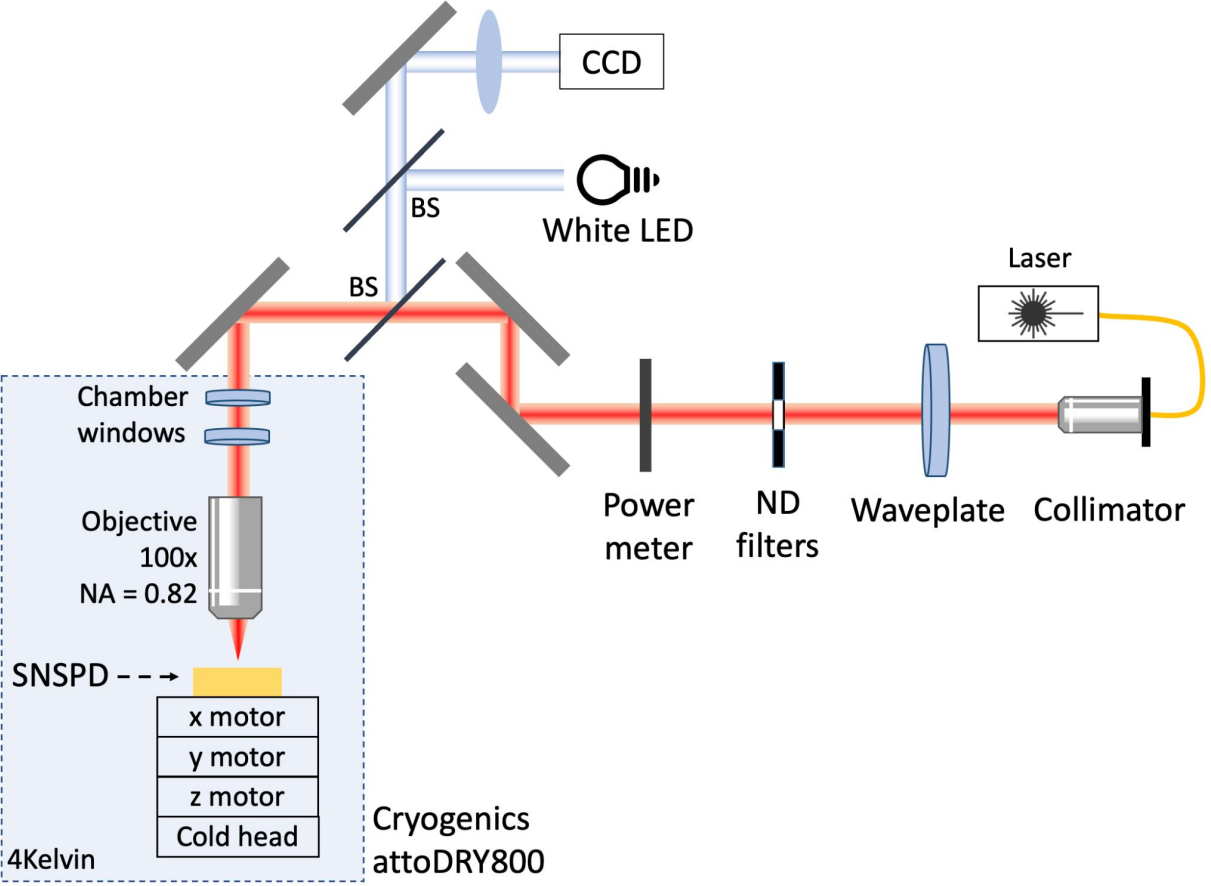
300K
Vacuum Shroud

40K
Cold Shield

4K
Sample Holder
with T-sensors & xyz motor



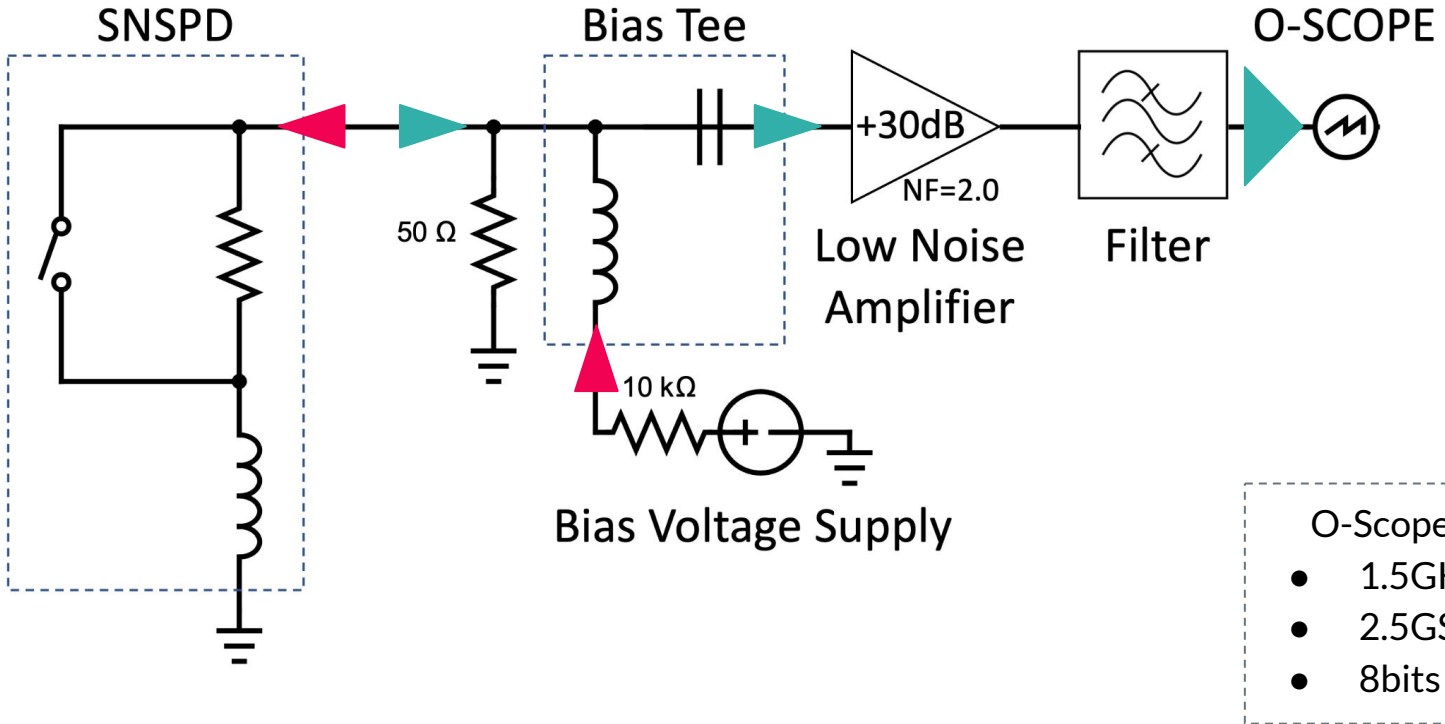
Optical Setup – Open-Air Coupling

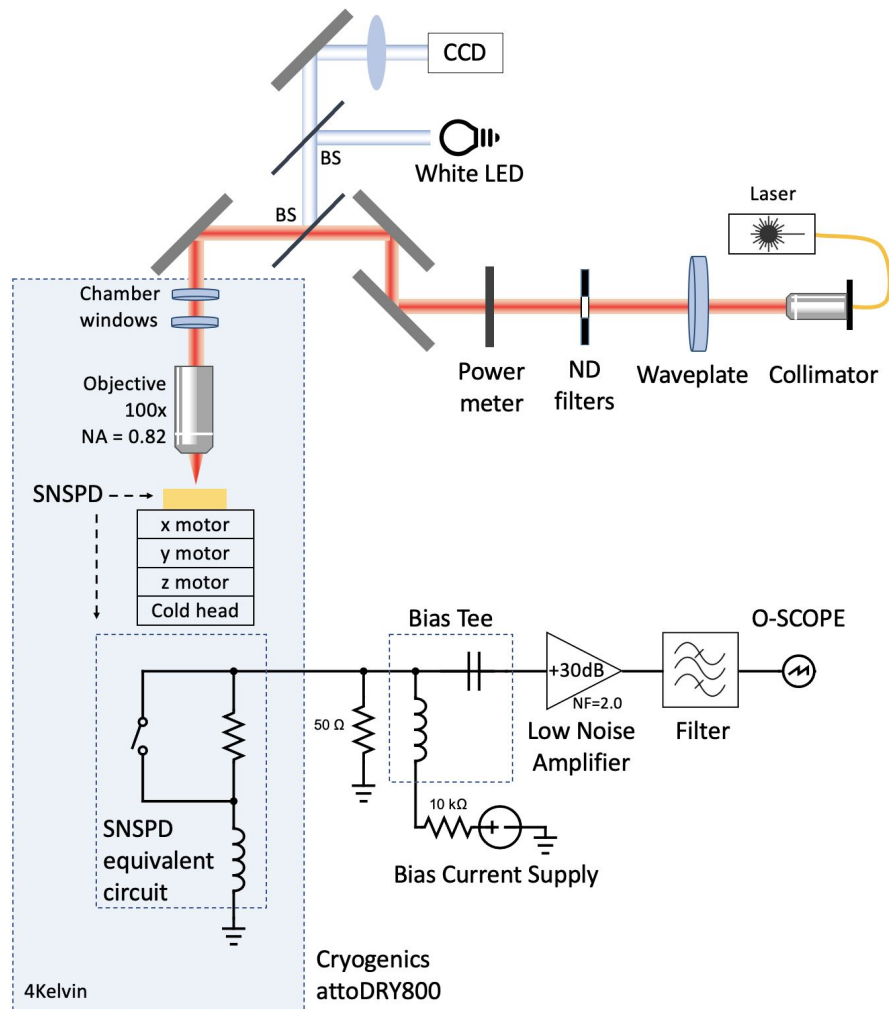


CCD Image



Electrical Setup





CW Laser Configuration

Laser

- 532nm CW
- 100 μ W

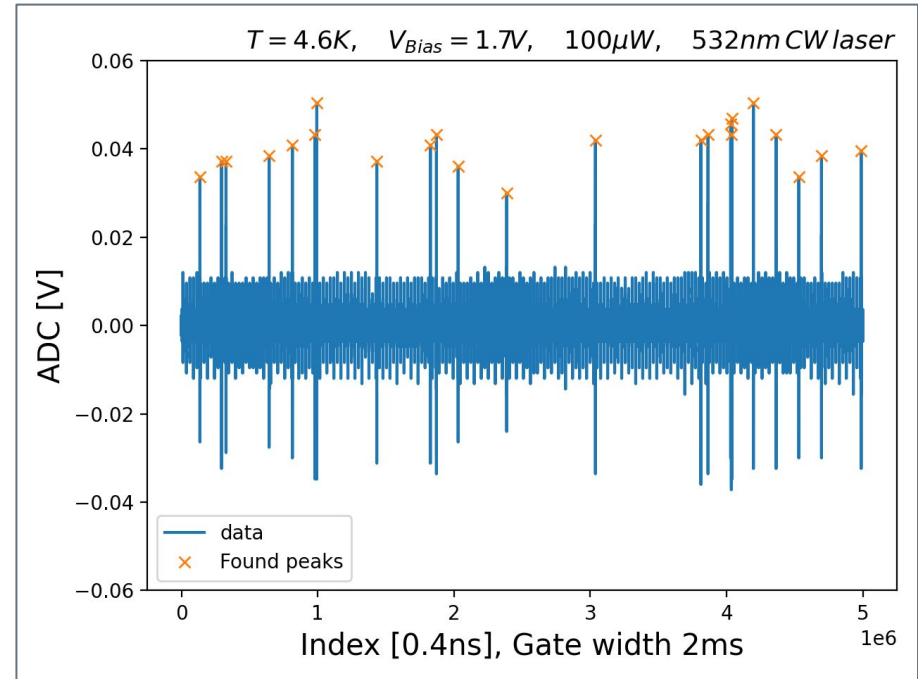
Oscilloscope

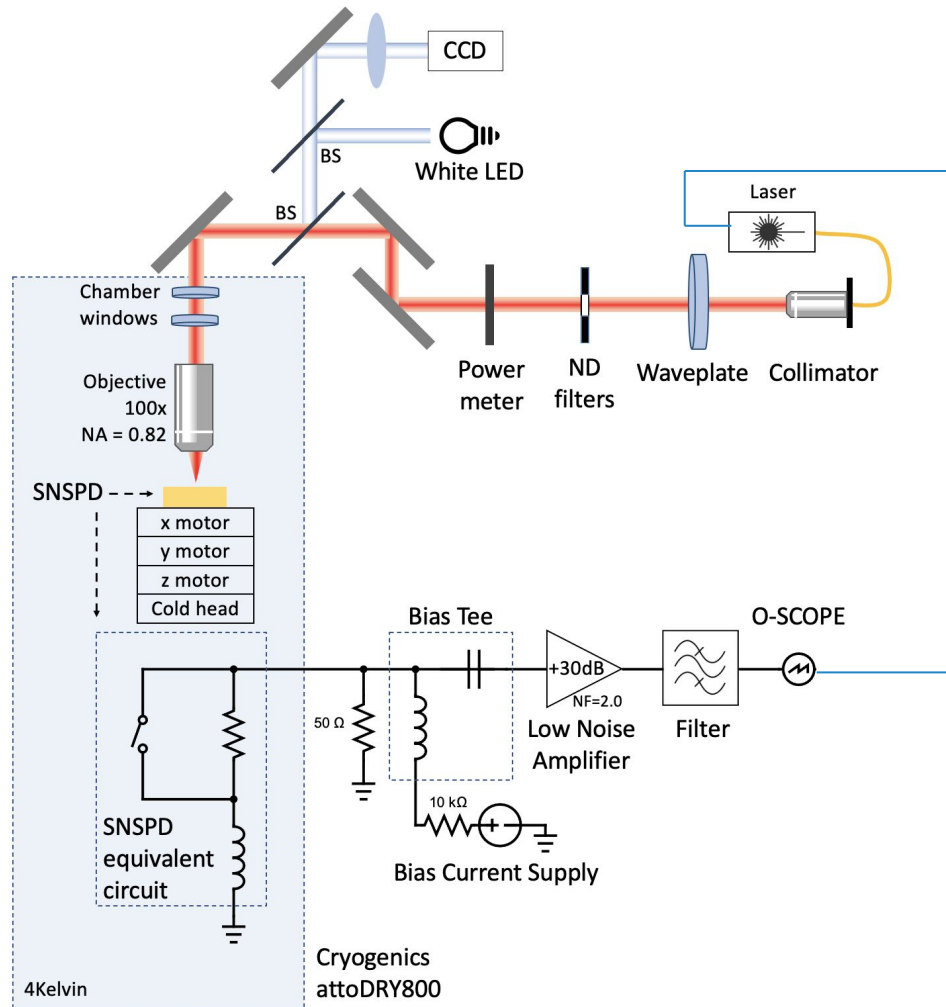
- Sampling Rate: 2.5GS/s (0.4ns)
- Time Gate: 5M Samples \rightarrow 2milisecond

Counting

- Peak finding
- Threshold: 20mV
- Peak Minimum Distance: 40ns

1 Oscilloscope Time Gate



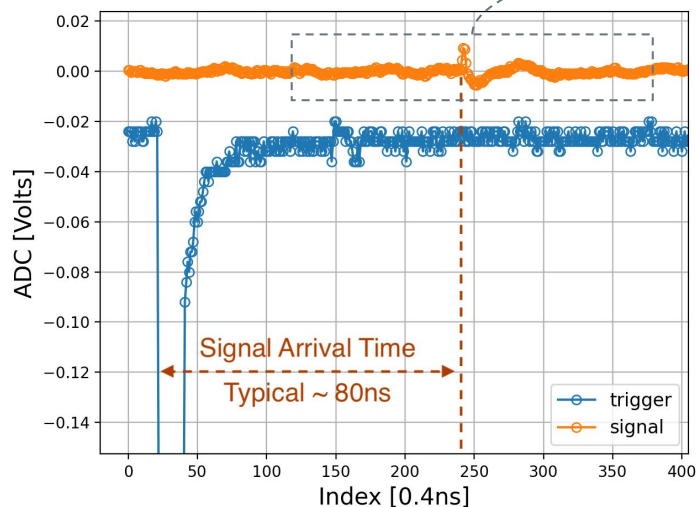


Pulsed Laser SYNC

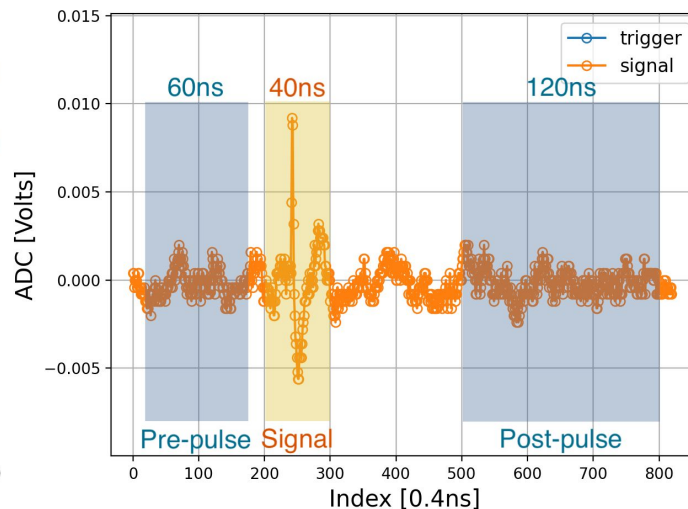
Pulse Data Taking

Pulse Laser Repetition Rate: 2.5MHz (400ns)
Pulse Laser Width: 100ps
Oscilloscope Sampling Rate: 2.5GHz (0.4ns)
Trigger: Laser Sync
Signal: Amplified SNSPD output

Event Display:



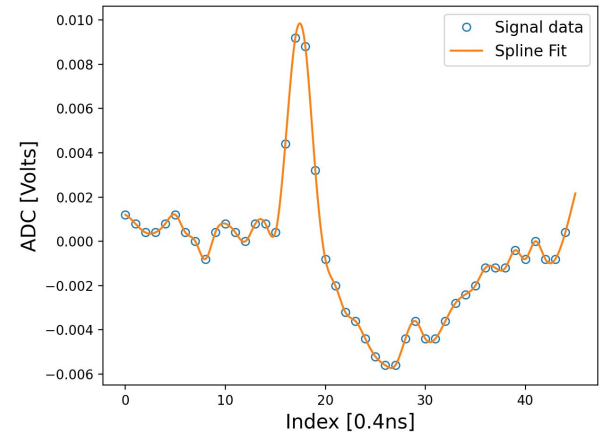
Sub-window of
1 Laser Trigger



Define Signal &
Sideband Region

Event Selection & Signal Reconstruction

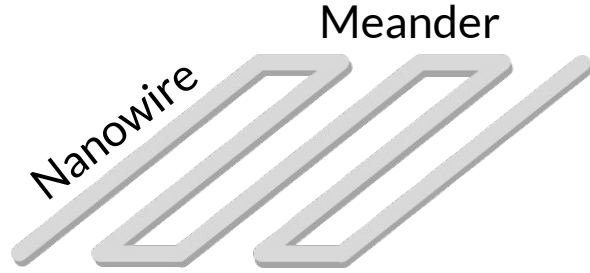
- Signal Reconstruction within the Signal Region
 - Cubic spline fit → turn the discrete data points into continuous function
 - Differentiate the spline function → Find turning points
- Variables
 - Amplitude = Voltage range (including overshoot)
 - Pulse arrival time = time of 50% voltage level of rising slope
 - Rise time = Time interval between 10%-90% of rising slope
- Event Selection
 - Signal Amplitude > 3mV
 - Voltage Differentiate at rising slope > 2mV/sample



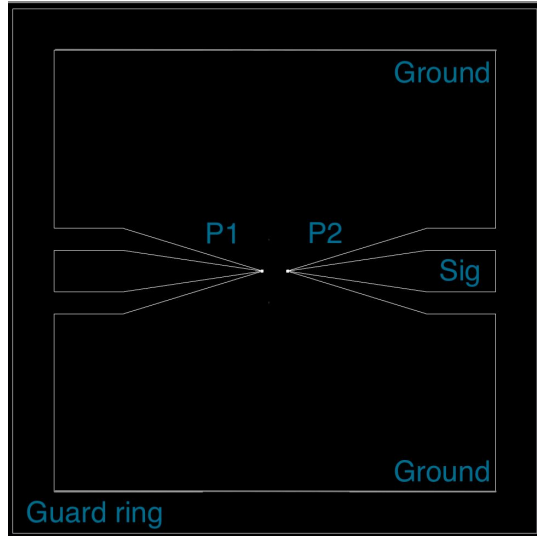
$$\text{Detection Efficiency} = \frac{N_{Event\ Selection}}{N_{Event\ PreSelection}}$$

SNSPD Characterization w/ 532nm Pulsed Laser

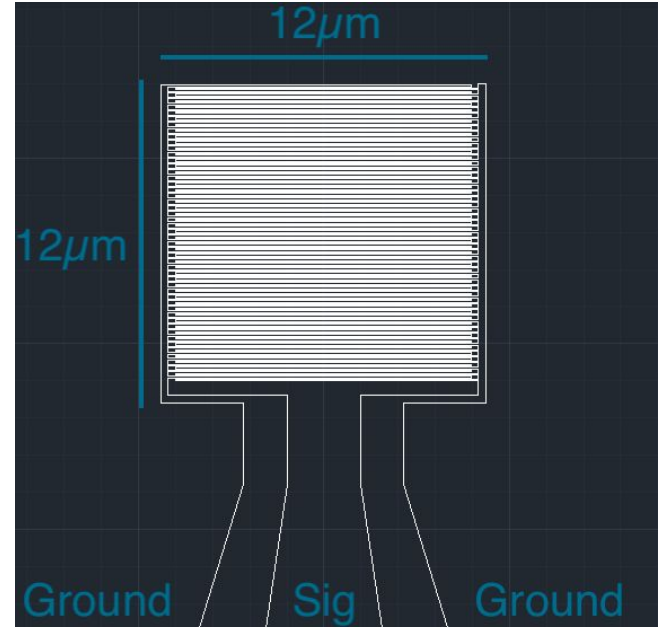
SNSPD Pattern Design



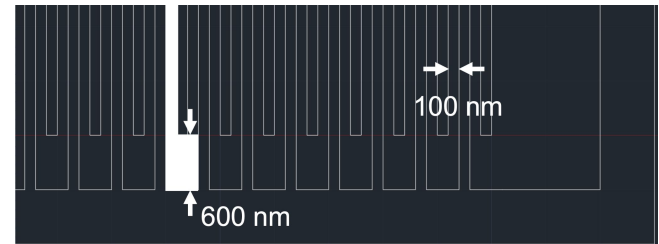
2 unit SNSPD with coplanar waveguide readout



Nanowire meander (Total Length 720 μm)

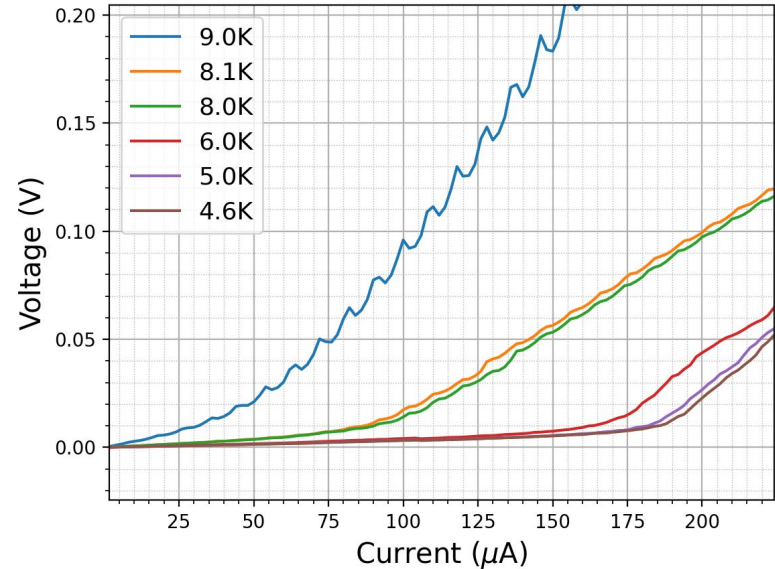
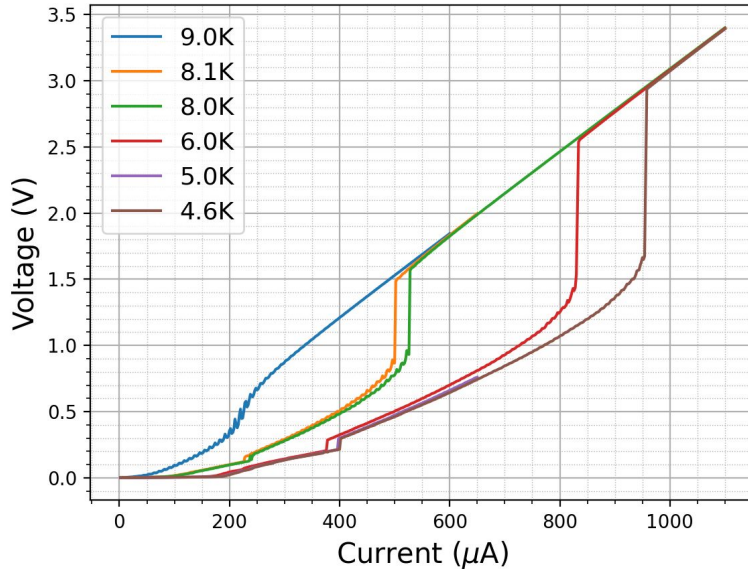


Width 100nm, Pitch 200nm



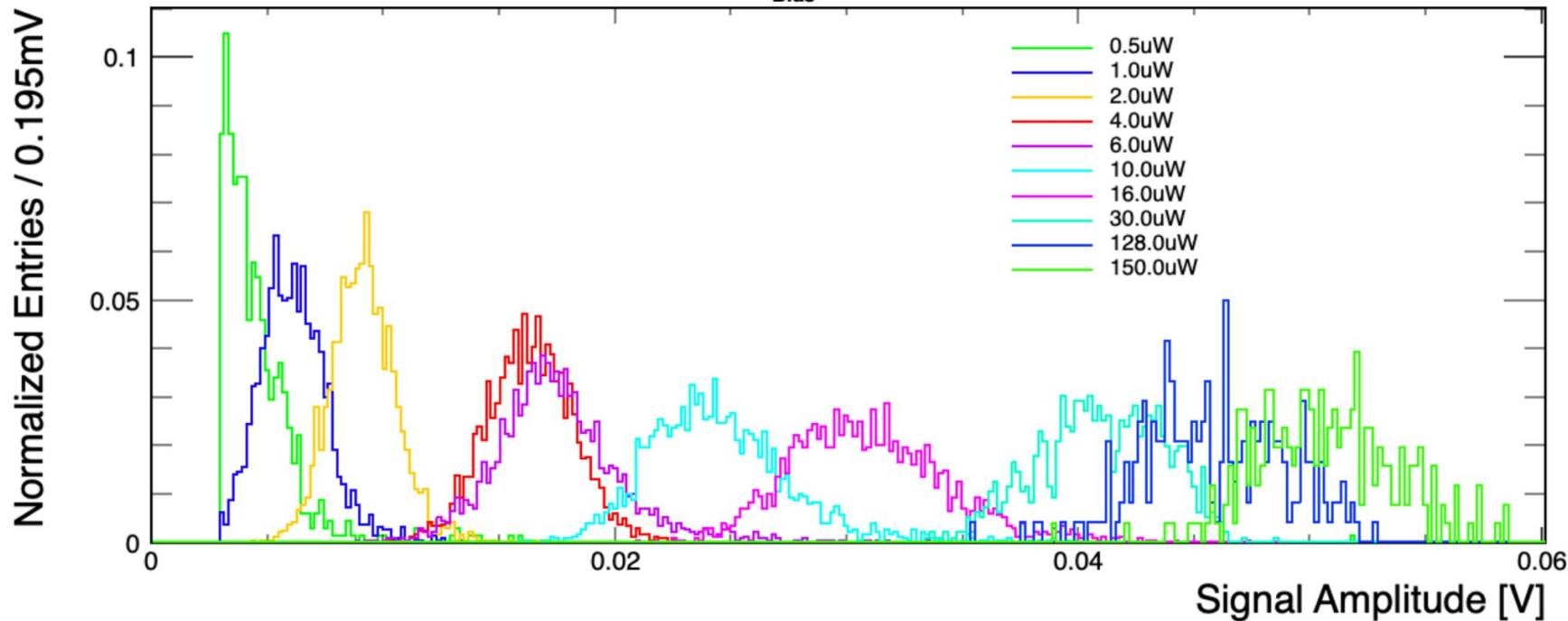
IV Curve

- Critical Current @ 4.6K ~ 180 μ A
- Critical Temperature ~ 9K
- Wide Transition Width ~ 800 μ A

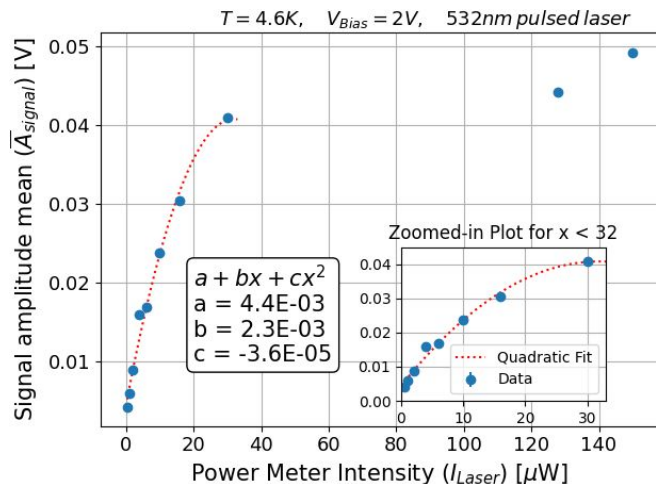


Laser Power Sweep

$T=4.6\text{K}$, $V_{\text{Bias}}=2\text{V}$, 532nm pulsed laser, 2.5MHz Repetition rate

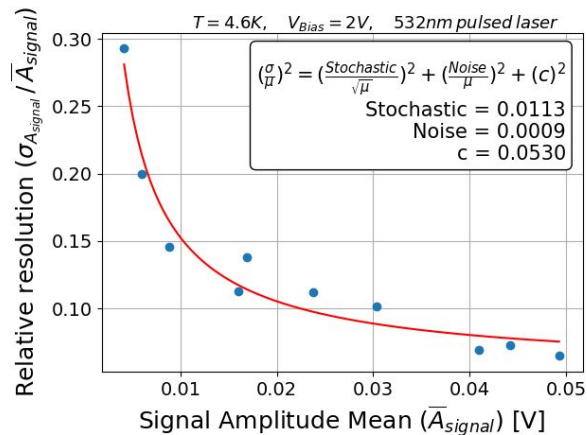


Preliminary Results

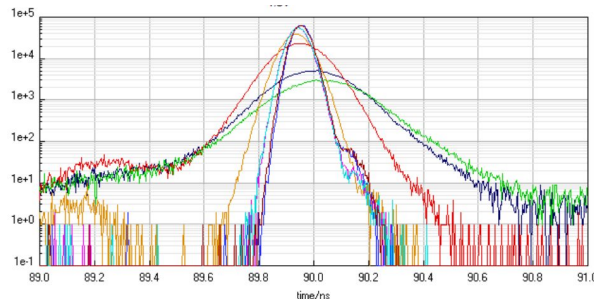


- $I_{\text{Laser}} < 30\mu\text{W} \rightarrow \bar{A}_{\text{signal}}$ has a quadratic gain
- $I_{\text{Laser}} > 30\mu\text{W} \rightarrow \bar{A}_{\text{signal}}$ slowly rises / saturates

Light Intensity Dependence!!



- 1% stochastic term
- 5% constant term



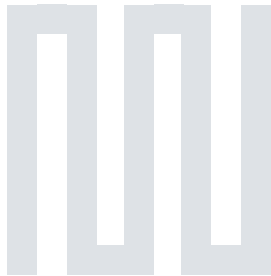
- TCSPC module (4ps)
- Time jitter $\sim 100\text{ps}$

SEM image

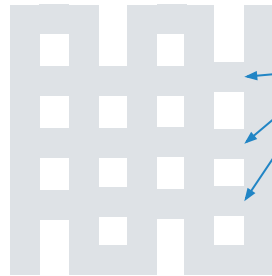
- Mesh-like structure
 - Nano-tunnels dimension around 10-100nm
 - Reason of the wide transition and kinks in IV Curve
 - Currently retuning EBL parameters

● This accident may lead us to SNPSD calorimeters!

- Very fast response (100ps level)
- Wide dynamic range
- Good energy resolution

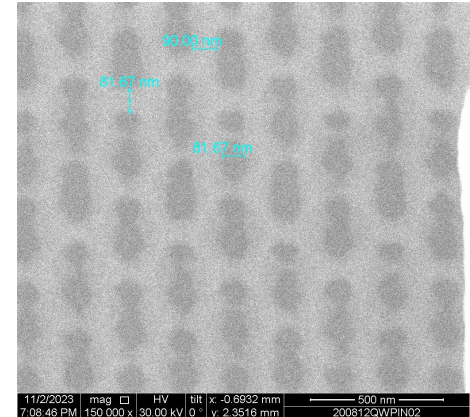
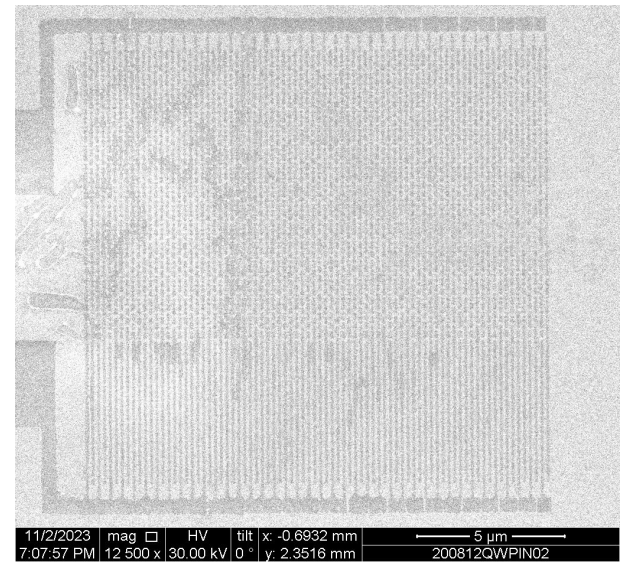


Original design



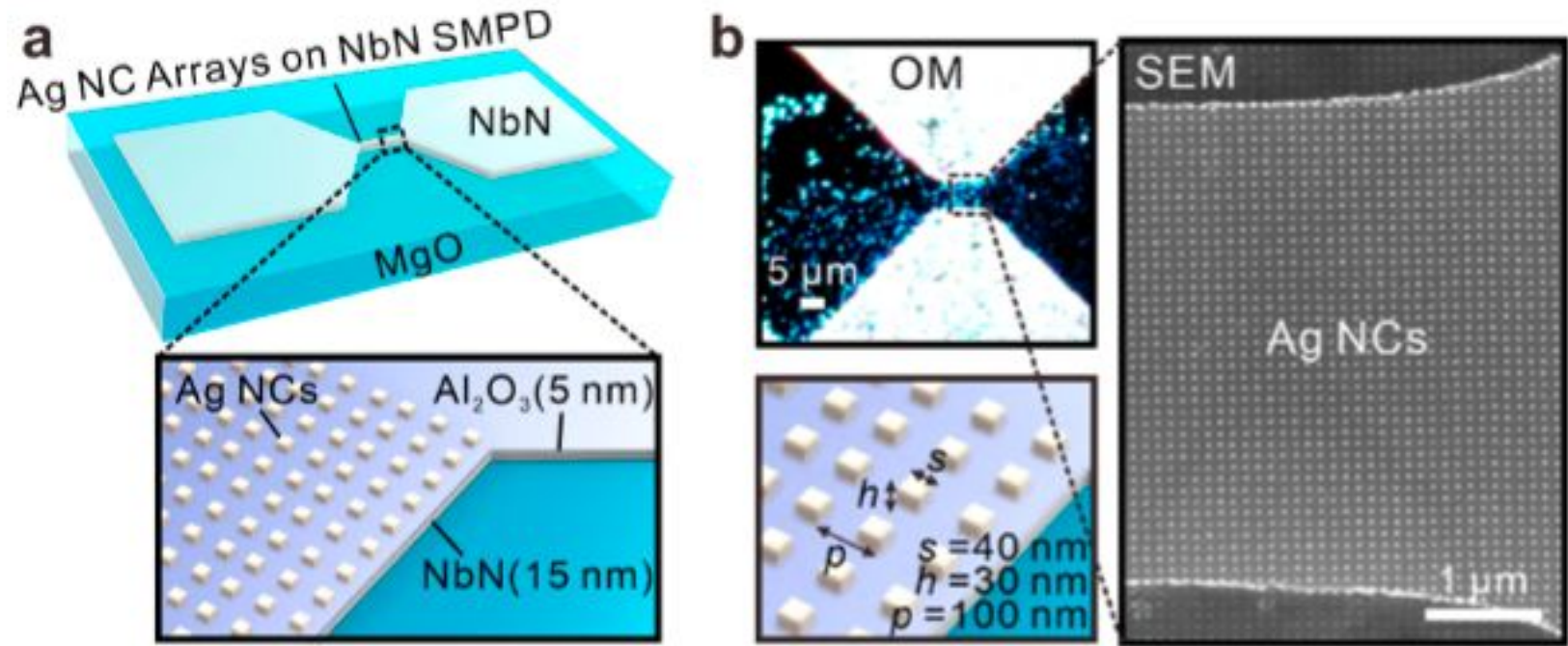
SEM image

nano-tunnels



Gap-plasmon Superconducting “Microwire” Single Photon Detector

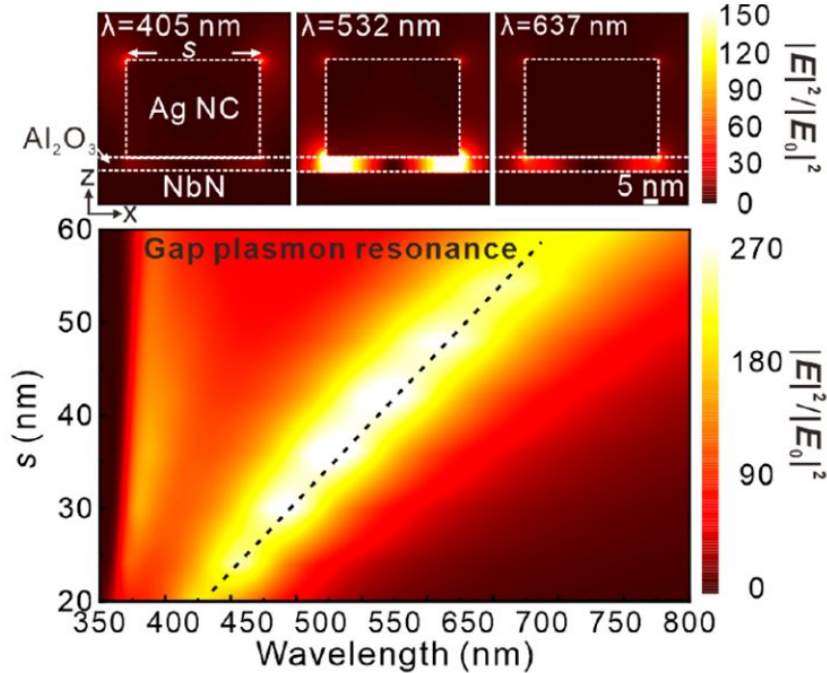
Gap-Plasmon-Enhanced SC Microwires



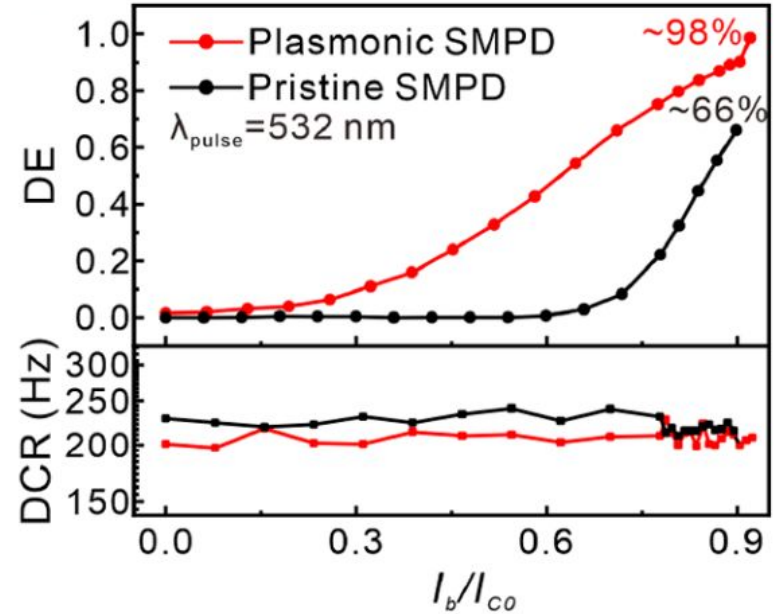
Yang, J.-W. et al. Nanoscale Gap-Plasmon-Enhanced Superconducting Photon Detectors at Single-Photon Level. Nano Lett. (2023).

Results

FDTD Simulation



Detection efficiency

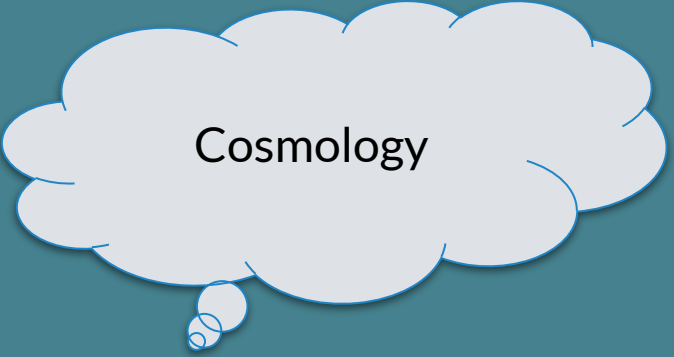


Gap-plasmonics nanocubes may lead us to sensitivity in longer wavelengths!

Why do we need SC
IR single photon detectors?



Particle Physics

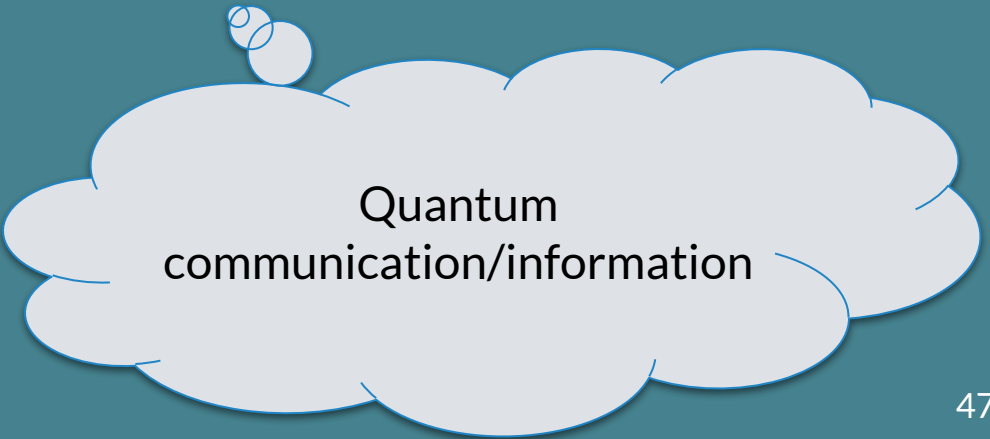


Cosmology

Wide variety of applications



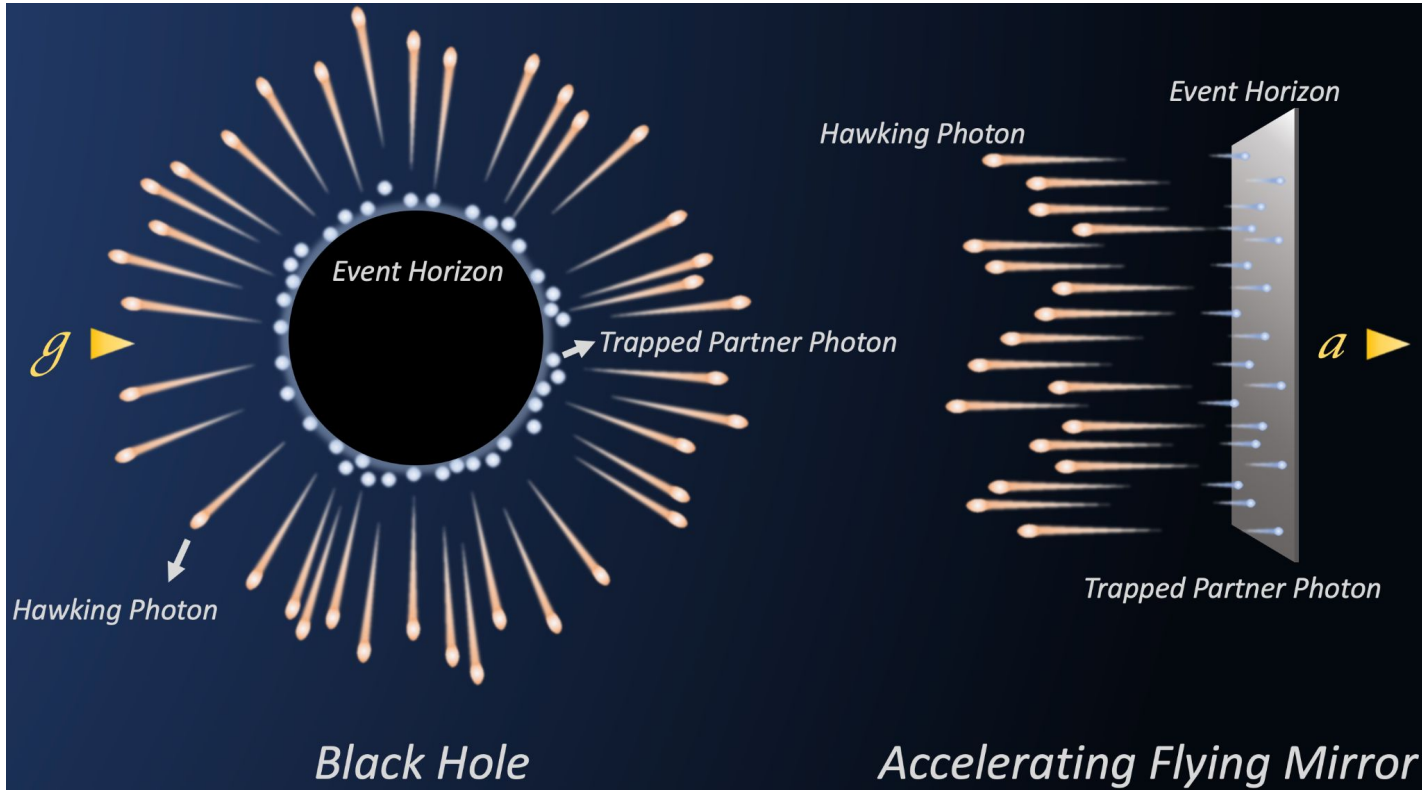
Astroparticle physics



Quantum
communication/information

Analog Black Hole

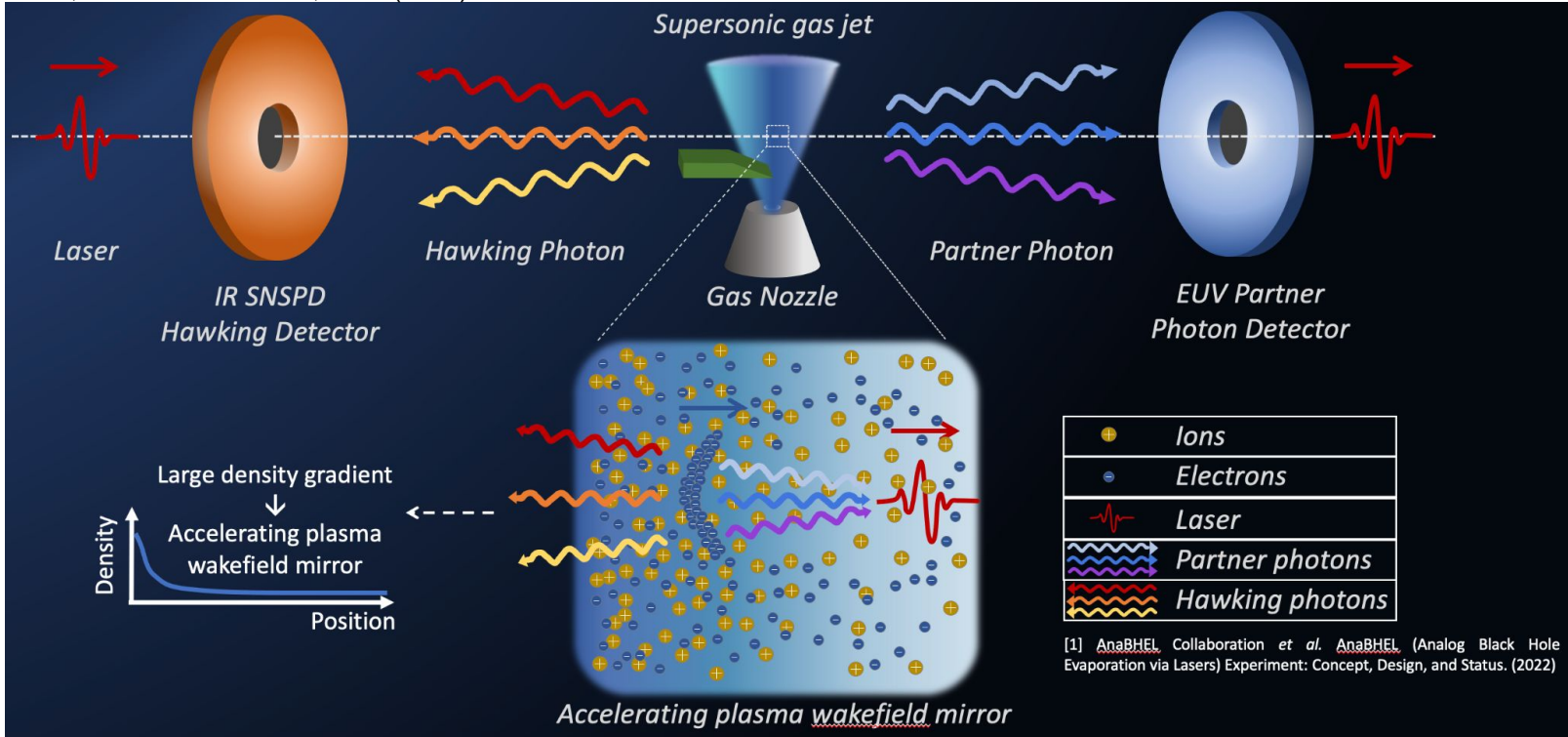
Chen, P. & Mourou, G. Phys. Rev. Lett. 118, 045001 (2017).



Equivalence Principle

AnaBHEL (Analog Black Hole Evaporation via Lasers) Experiment

Chen, P. et al. Photonics 9, 1003 (2022).



Requirements:

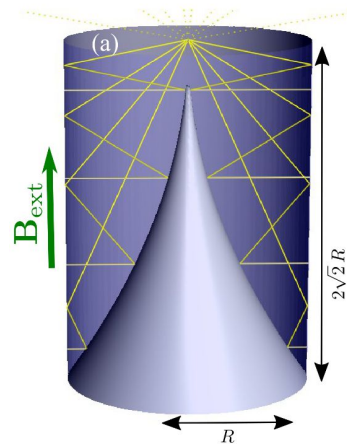
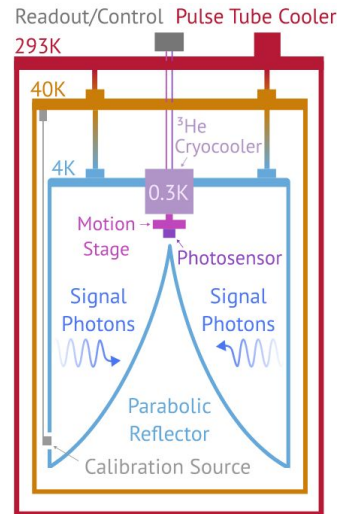
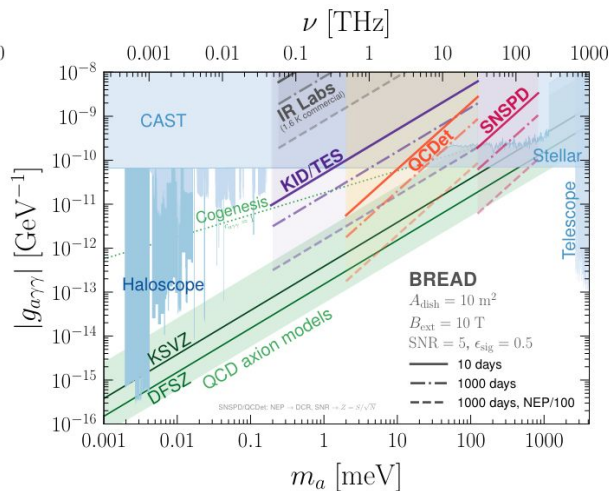
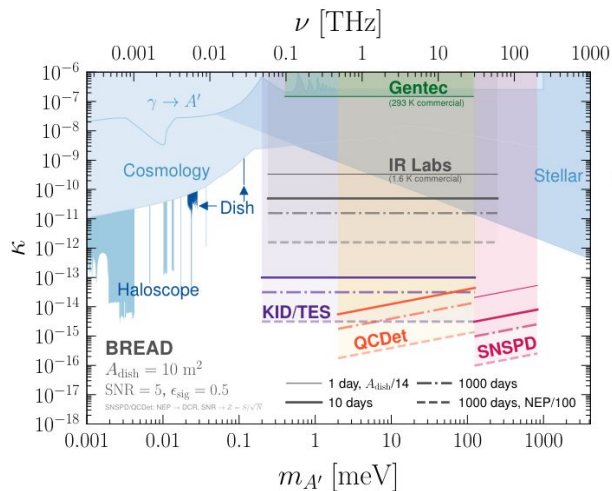
- Broadband 10-100 μ m single photon sensitivity
- High efficiency, High speed, Low Timing Jitter, Low Dark Count
- Polarization distinguishability

Dark Matter Searches

- Dark matter candidates with $m_{\text{DM}} < 1 \text{ eV}$
 - QCD Axions (a)
 - Dark Photons (A')
- Non-zero DM-photon couplings \rightarrow lab detection through EM interactions

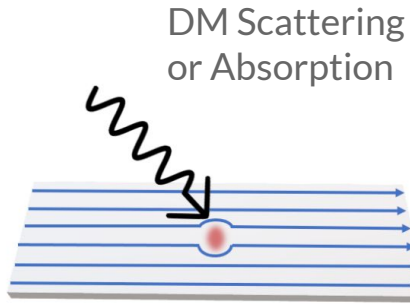
Broadband solenoidal haloscope for terahertz axion detection (BREAD)

Phys. Rev. Lett. 128, 131801 (2022).

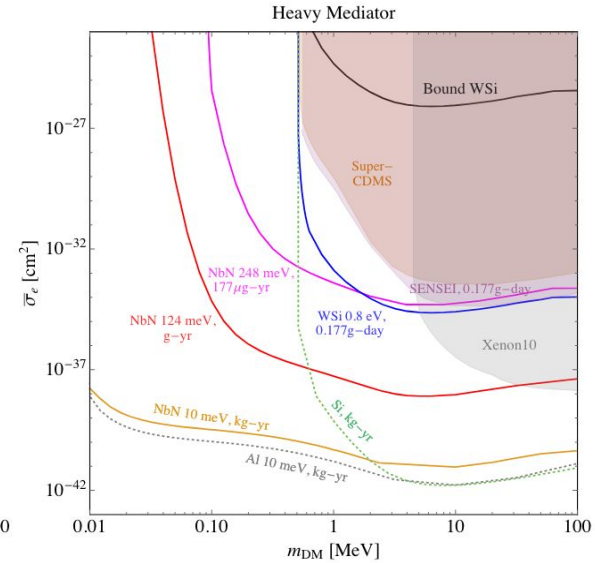
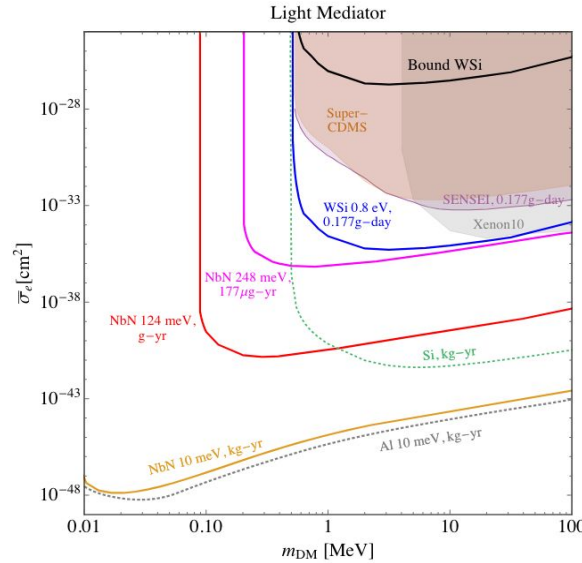


Dark Matter Searches – Direct interaction

Phys. Rev. Lett. 123, 151802 (2019).



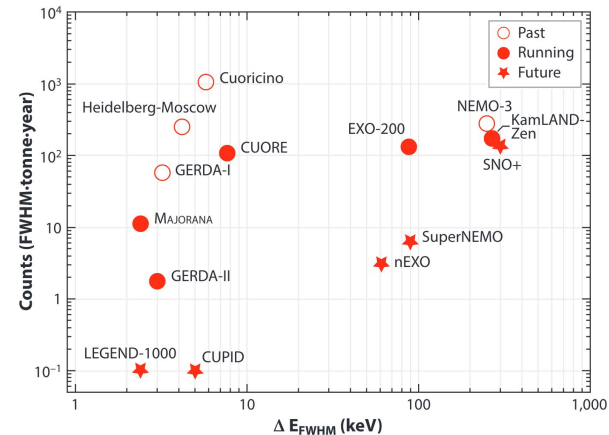
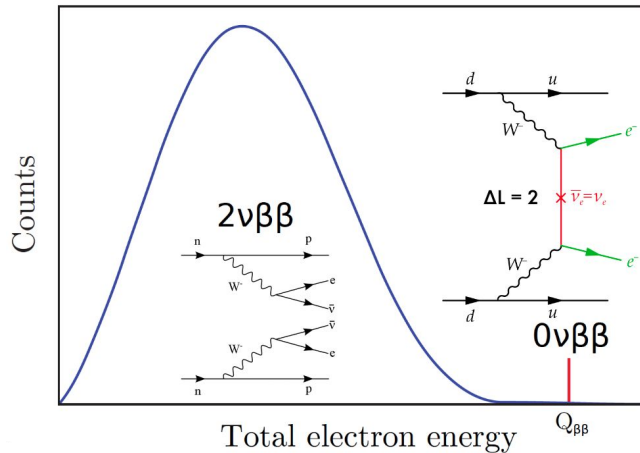
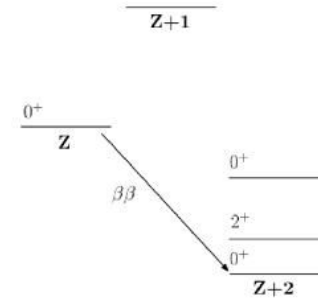
- Requires stable and low Dark Counts



Lower energy/wavelength threshold can lead to larger DM detection phase space!

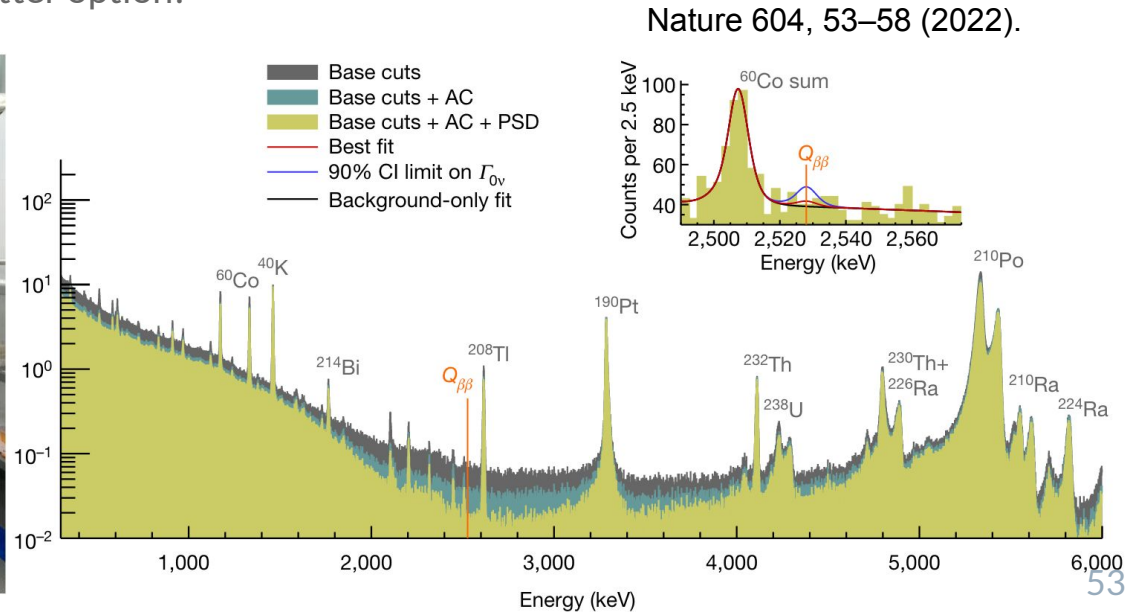
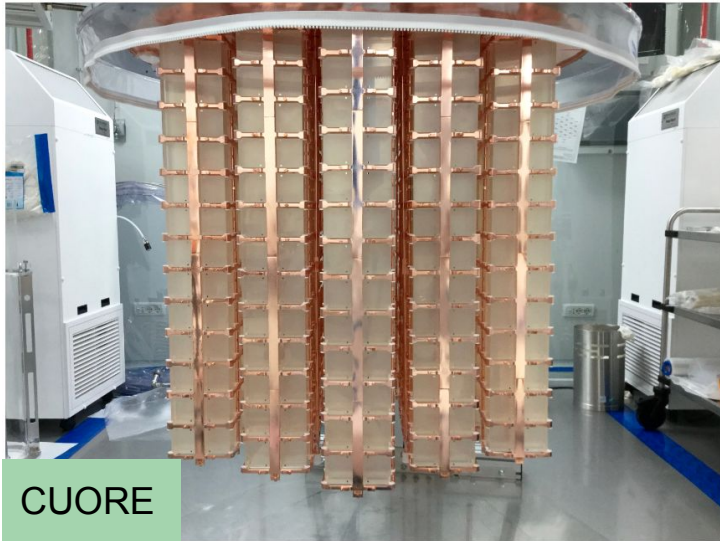
Neutrinoless double beta decay

- $2\nu\beta\beta$ is a rare SM radioactive decay process
- $0\nu\beta\beta$ is a theoretical, experimentally unobserved process
- Implies $\Delta L \neq 0$
 - Lepton number violation = new physics!
 - Prove the Majorana nature of neutrino \rightarrow Majorana mass
 - Connection to baryon asymmetry



Neutrinoless double beta decay

- Planning upgrades: CUPID-1T
 - 1 Ton of ^{100}Mo
 - Irreducible background from $2\nu\beta\beta \rightarrow$ Pileup becomes important with large amount of source
 - Implementation of TES \rightarrow Low Dark Count, 10us timing resolution, good energy resolution
- SNSPD calorimeter may be an even better option!

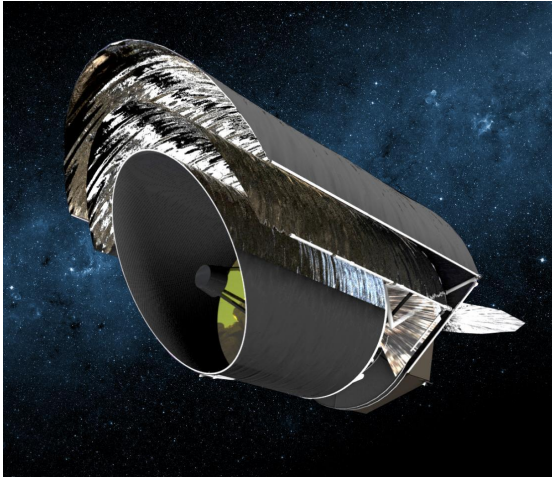


Exoplanet search

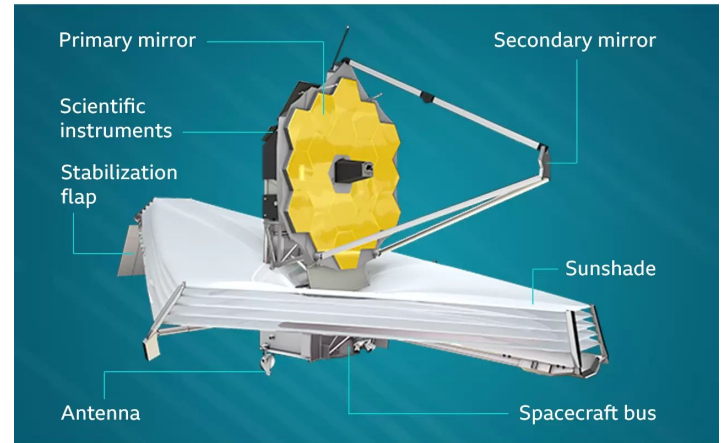
JATIS 7, 011004 (2021).

- Planetary science (Outside the solar system)
- Search for Earth-like, habitable planets
- Future: Origins Space Telescope (OST) (2035)
 - Targetting mid to far-infrared (5-600 μm)
 - Actively cooled to 4.5K \rightarrow SC detectors

Origins Space Telescope Proposal

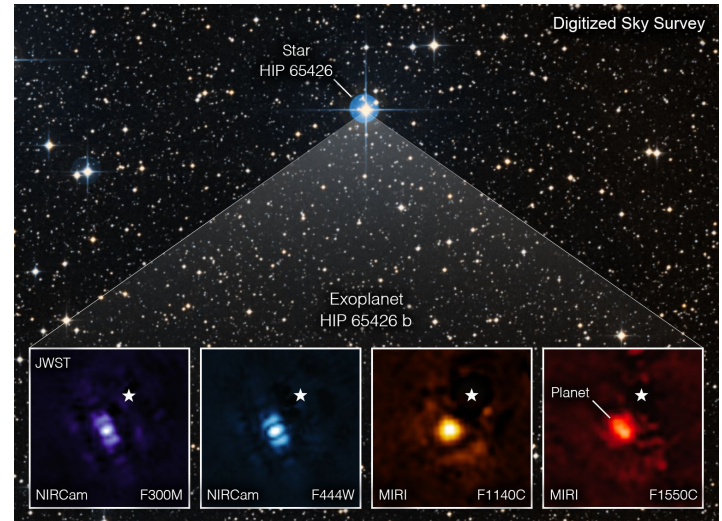


James Webb Space Telescope



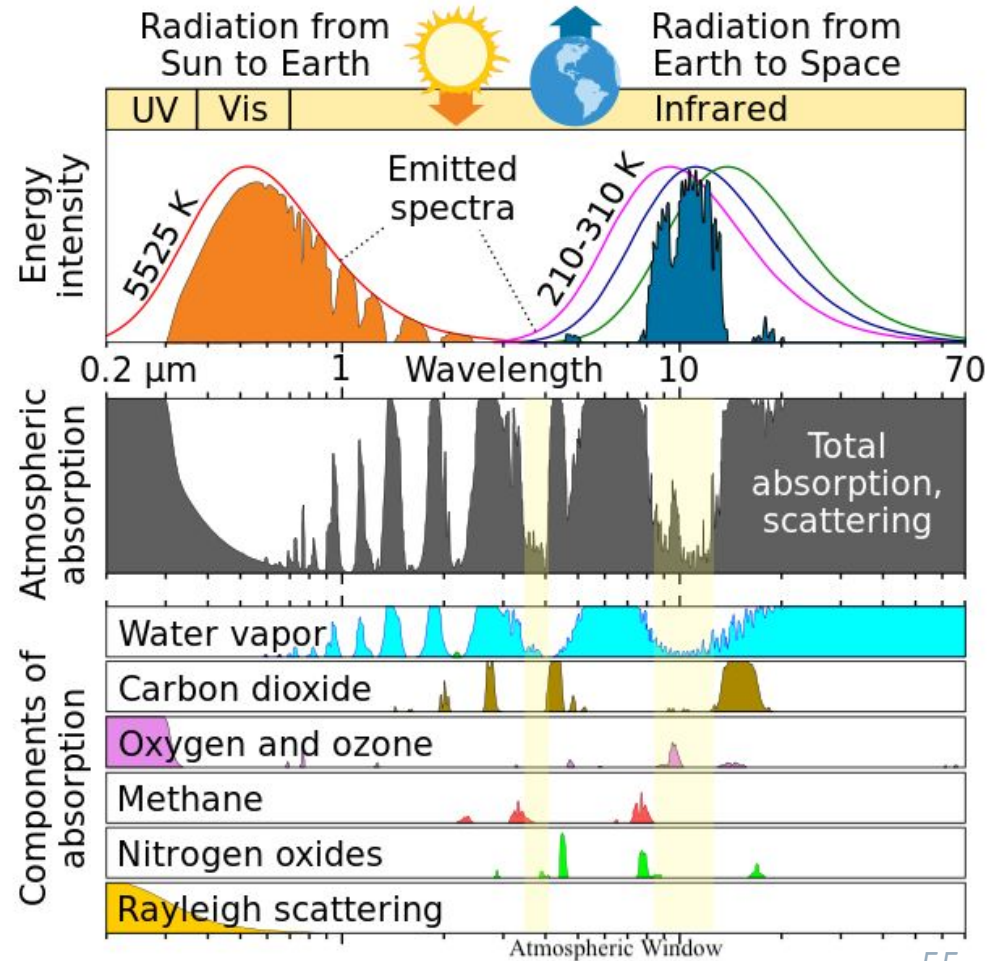
Source: Nasa

B B C



Atmospheric Window

- No sun radiation & atmospheric absorption
- At around 3-4 μm & 8-10 μm
- Ground-to-Satellite/Space Applications
 - Free space optical (FSO) communication
 - Quantum secure keys
 - Space Observatory

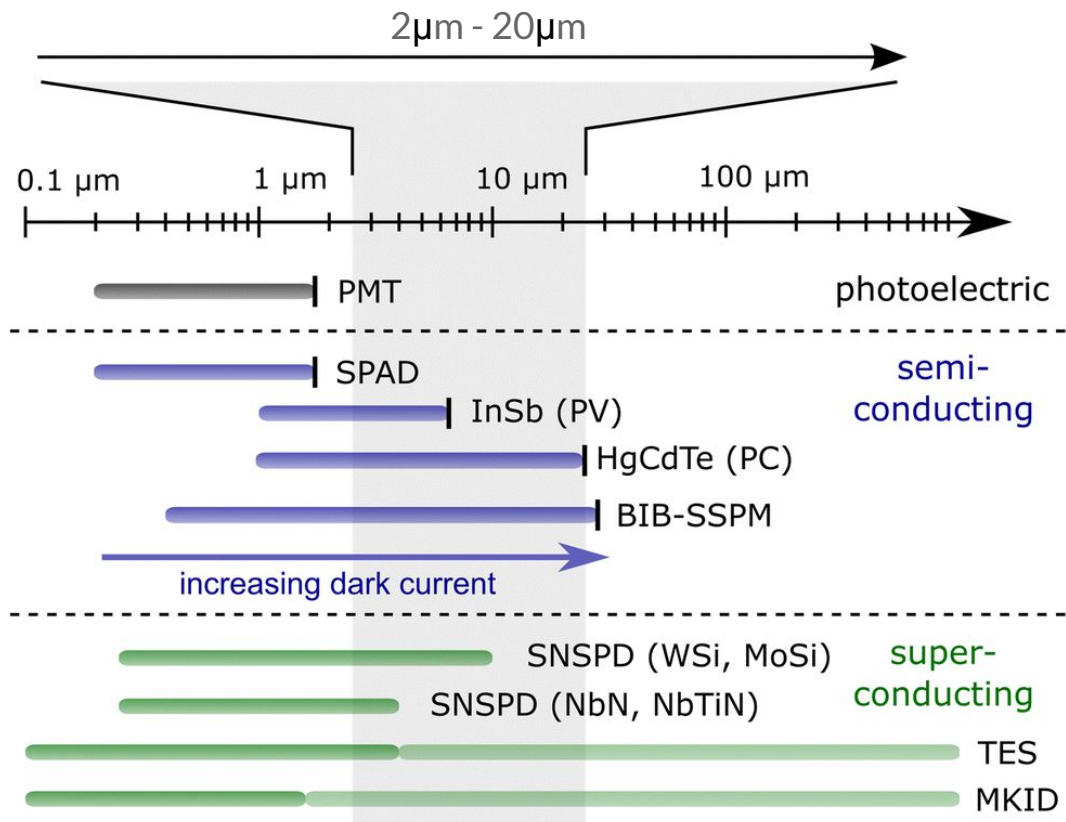


Comparing SC Single Photon Detectors @1550nm

Figure of Merit	SNSPD	TES	MKID	STJ
Efficiency	99.5%	98%	17%	20%
Number resolution	5	29	7	/
Recovery time	80ps	75ns	50 μ s	20 μ s
Timing jitter	2.6ps	30ns	1 μ s	1 μ s
Dark counts (Hz)	0.01	0.0086	/	/
Maximum count rate	1.5x10 ⁹	10 ⁵	2x10 ³	10 ⁴
Number of "pixels"	1024	36	20440	120

Optimal detector for quantum communication with fiber optics

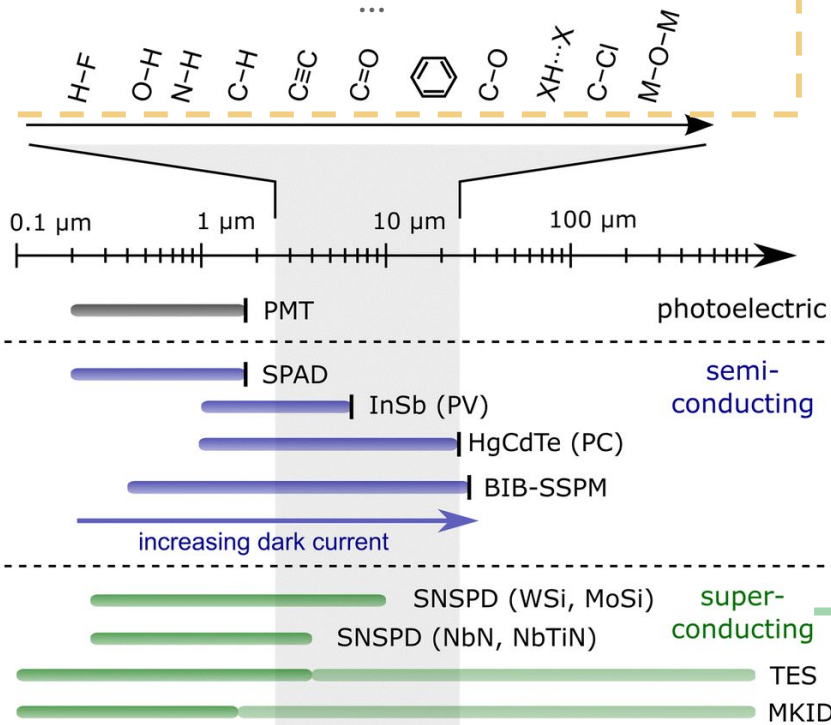
Wavelength Sensitivity Range Comparison



Chemical Society Reviews 52, 921–941 (2023).

Quantum Communication @ Atmospheric Window

Analog Black Hole
Exoplanet Search
Dark matter search



Mid - Far Infrared is a golden wavelength band for next generation measurements!

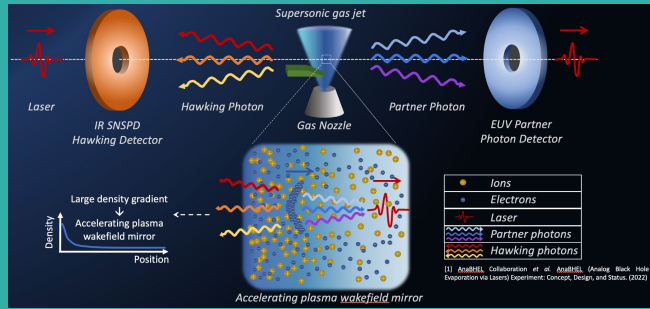
SNSPD can be the detector to meet all stringent requirements in these applications

Shown sensitivity in MIR
Potential calorimetry
Very fast timing
Low dark count

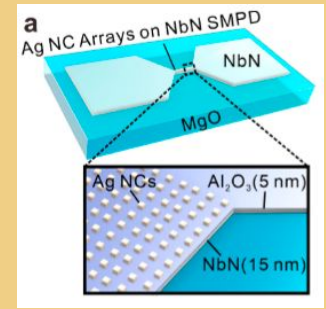
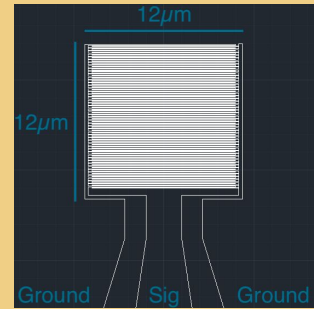
...

Chemical Society Reviews 52, 921–941 (2023).

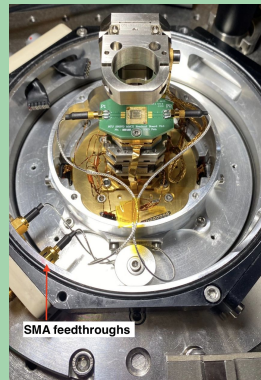
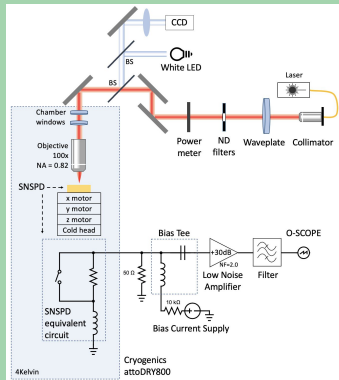
Applications



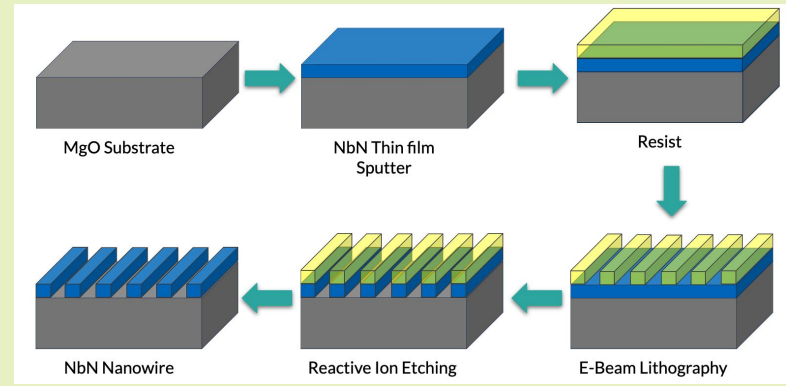
Design and simulation



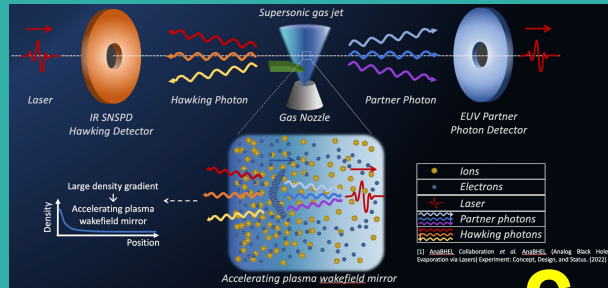
Characterization



Fabrication

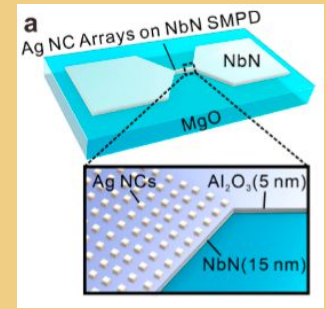
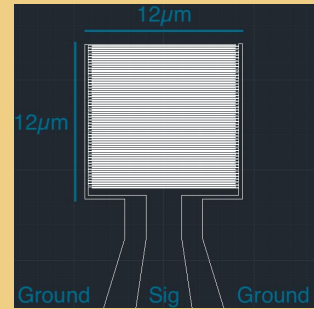


Applications

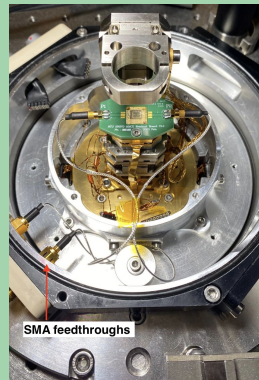
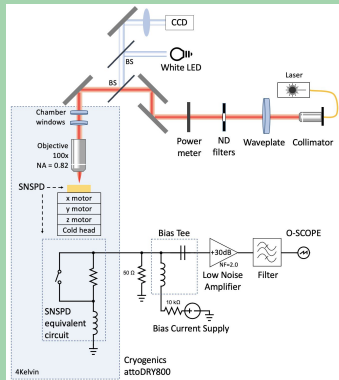


& More!

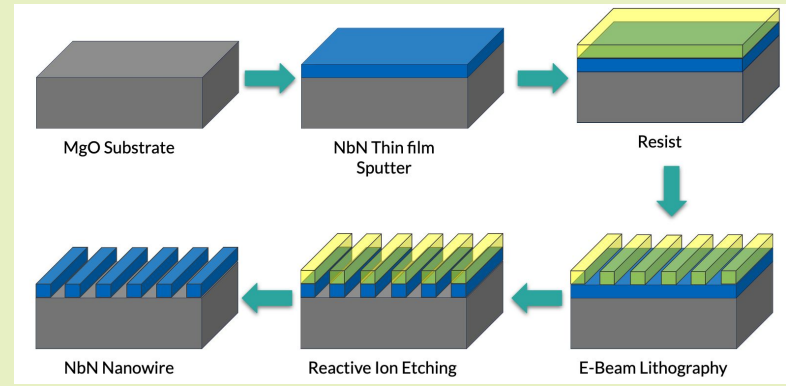
Design and simulation



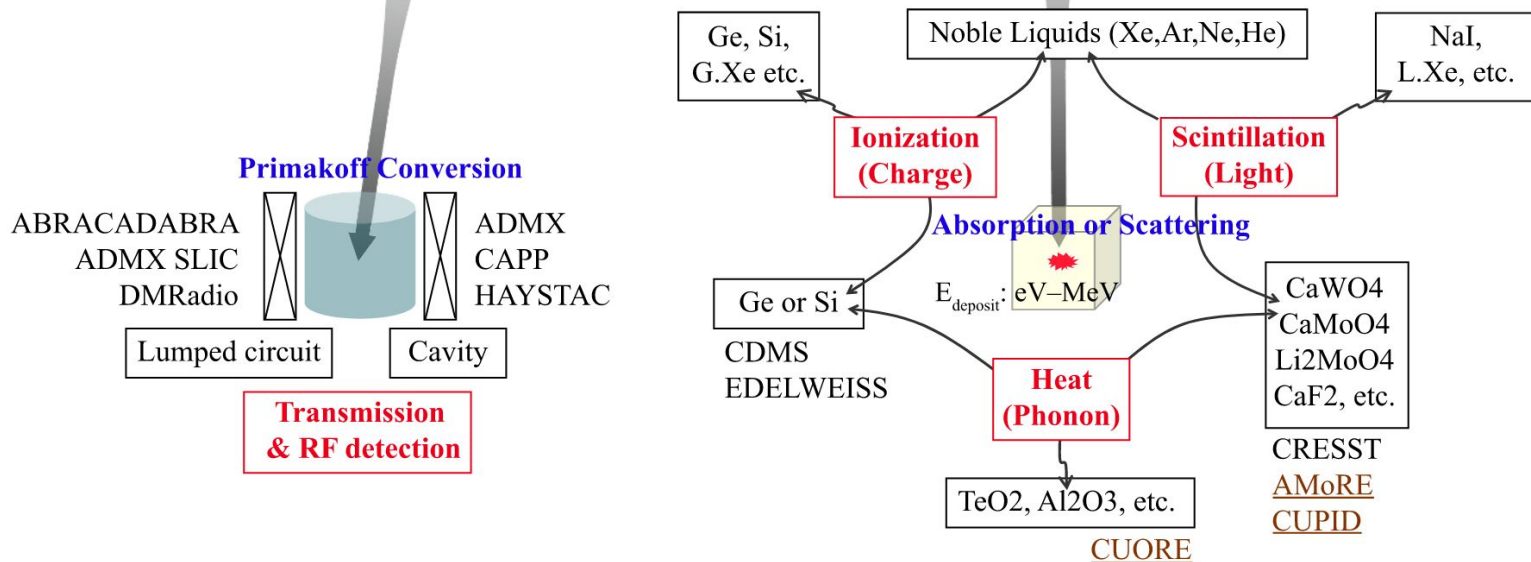
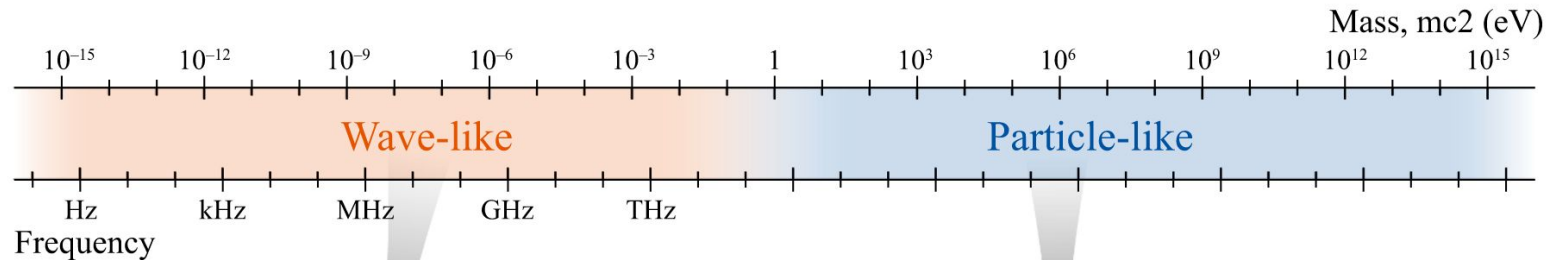
Characterization



Fabrication



Extra Slides

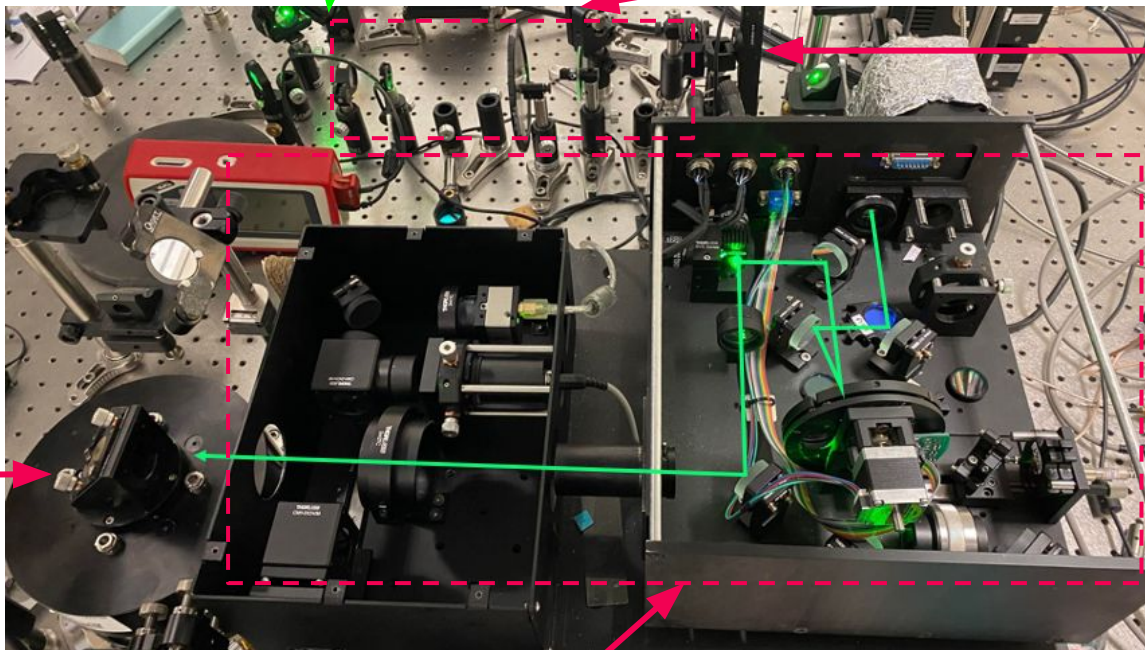


(1) Lasers:
Switch input source manually
with blocks and mirrors

(2) ND Filters Series:
Including fixed & variational ND filters

(3) Optical power meter:
Mounted on a 90°
Manual Flip Mount

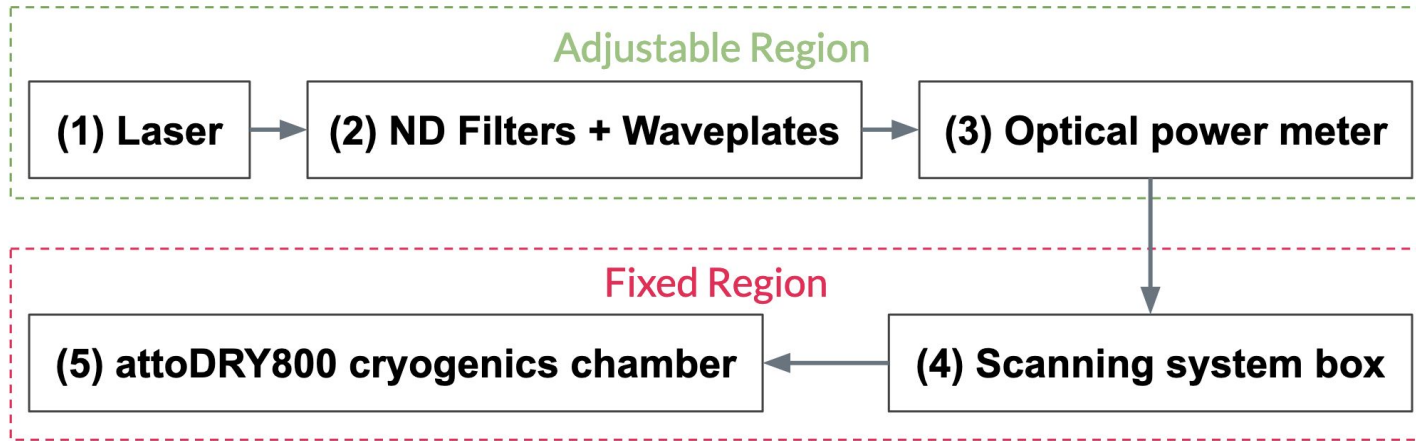
(5)
attoDRY800
cryogenics
chamber



(4) Scanning system box
(actual use irrelevant to us, but it contributes to power attenuation)

Transmission Factor Tests

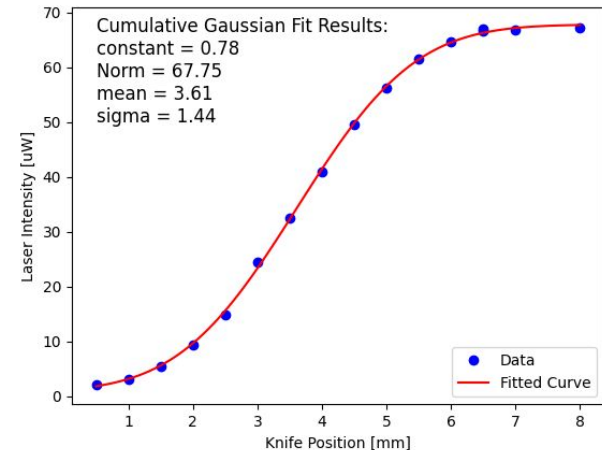
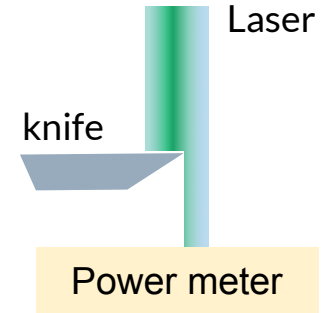
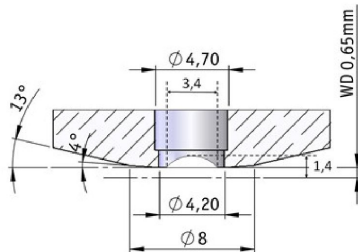
$$P_{\text{sample}} = P_{\text{laser}} \times T_{\text{total}}^{\lambda} = P_{\text{Power meter}} \times T_{\text{Fixed Region}}^{\lambda}$$



$$T_{\text{Fixed Region}} = T_{\text{ScanningBox}} \times 2T_{\text{window}} \times T_{\text{objective lens}} \times A_{\text{objective lens}} \times A_{\text{sample}}$$

Laser beam size - Knife Edge technique

- Laser beam size is broadened by a laser beam expander in the black box. The size will be larger than the objective lens clear aperture, so laser will be blocked partially
Currently the expander is fixed and cannot be removed.
- LT-APO/VIS/0.82 Objective lens apperture : 4.7mm
- Assuming the laser is collimated to the center of the objective lens
→ Laser within apperture 4.7mm ($\pm 1.63\sigma$) : 89.68%



Transmission calibration

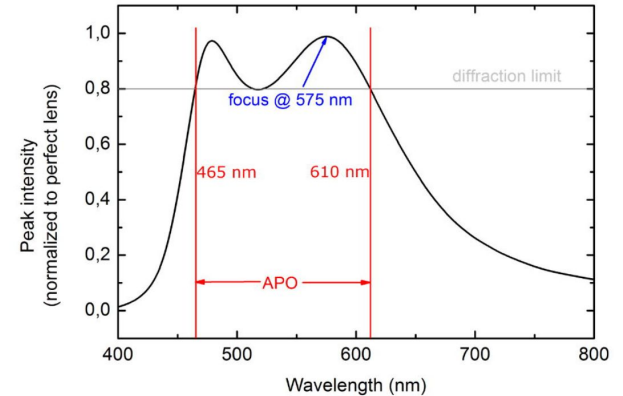
- $T_{\text{black box}}$ calibrated with 532 pulse laser \rightarrow 80%
- $T_{\text{Objective lens}}$ from spec @~532 \rightarrow 80%
- T_{Window} 90% at visible light
- A_{sample} corresponds to how well we focus the laser to the sample. Since the Rayleigh length after the objective lens is very short (several nm) and we see a clear image of the laser beam focused in the center of the sample \rightarrow We assume now that A_{sample} is 1

$$T_{\text{chamber + black box}} = T_{\text{black box}} \times 2T_{\text{window}} \times T_{\text{objective lens}} \times A_{\text{objective lens}} \times$$

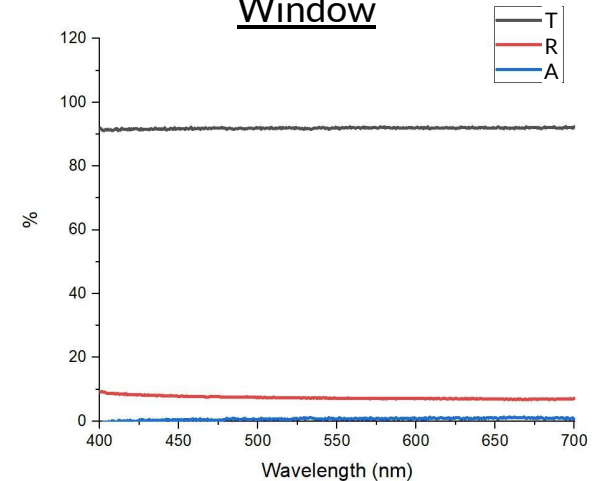
$$A_{\text{sample}}$$

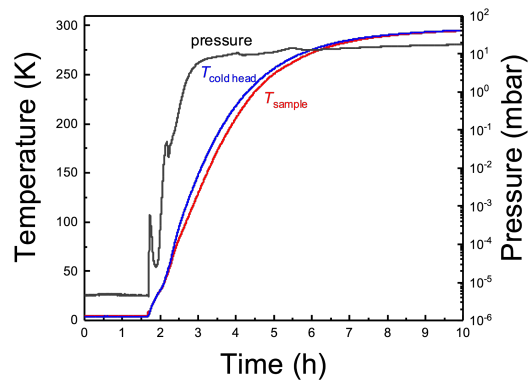
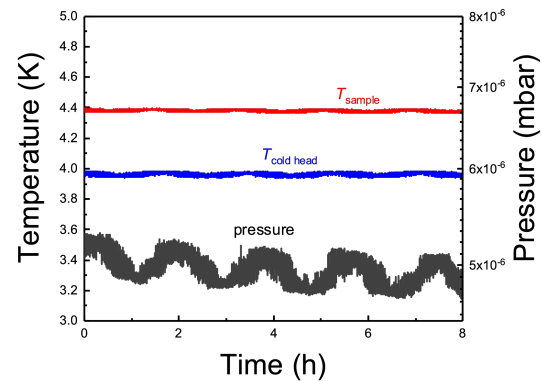
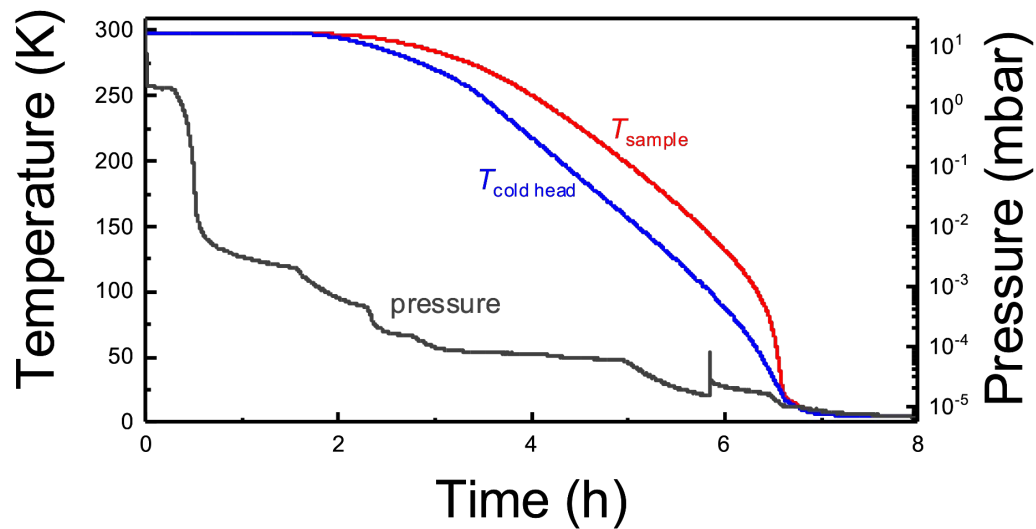
$$\rightarrow T_{\text{chamber + black box}} = 46\%$$

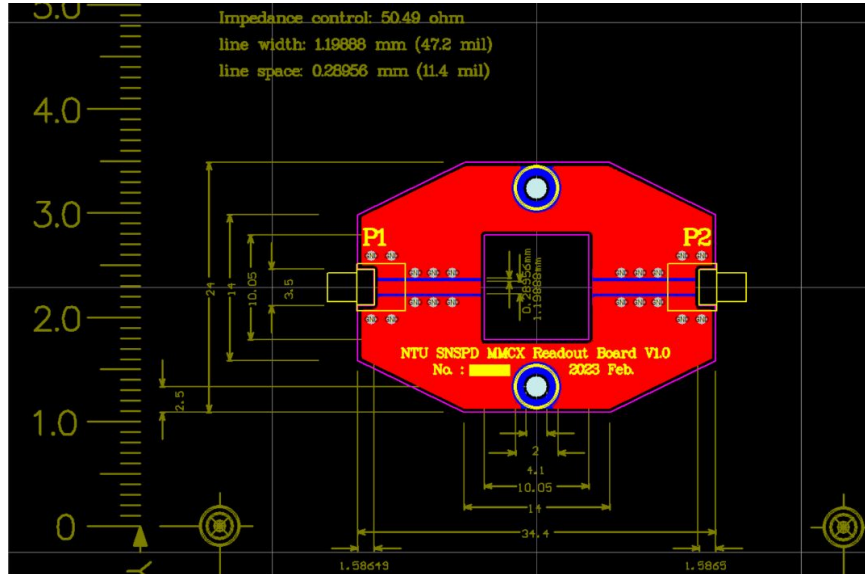
Objective lens



Window



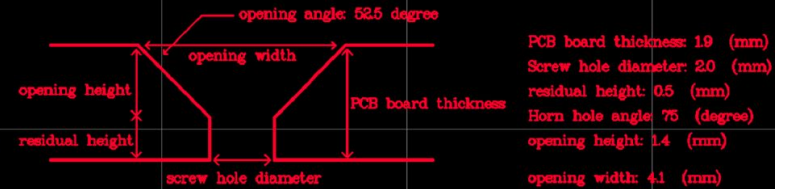




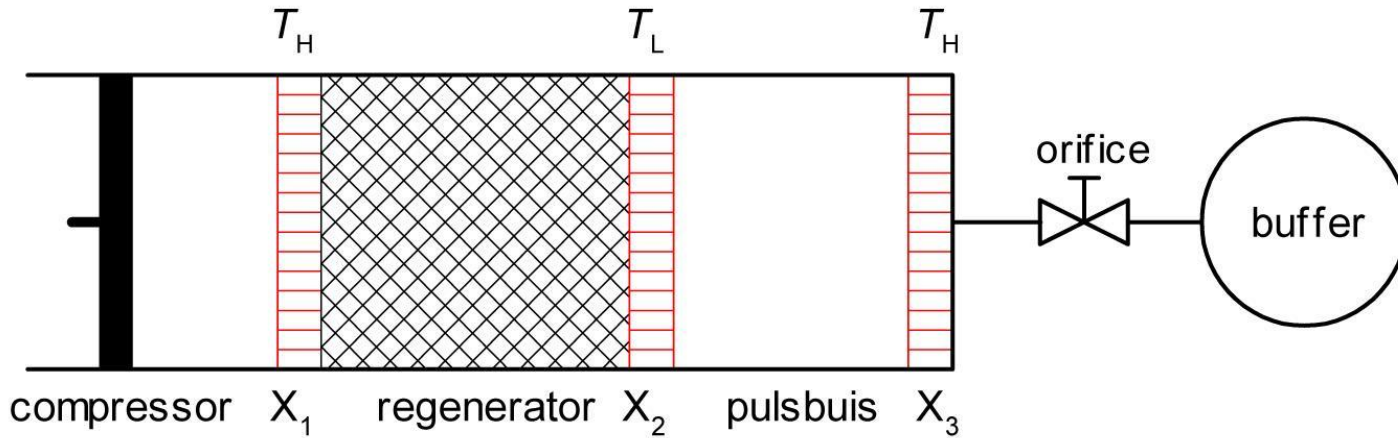
Layer Stackup Instructions

Layer	Stackup	Cu	Material	Thickness
			solder mask	0.7 mil
L1	Top layer	1.0 oz	Cu+Plating	1.6 mil
			Prepreg	6.2 mil
			Core	67.8 mil
			Prepreg	6.2 mil
L2	Bottom layer	1.0 oz	Cu+Plating	1.6 mil
			solder mask	0.7 mil
Overall Thickness				74.8 mil
				1.90 (mm)

Instructions for making flat head screw holes (2mm, NPTH, 2 pcs):



Pulsetube



By I, Mbeljaars, CC BY-SA 3.0,
<https://commons.wikimedia.org/w/index.php?curid=2222016>

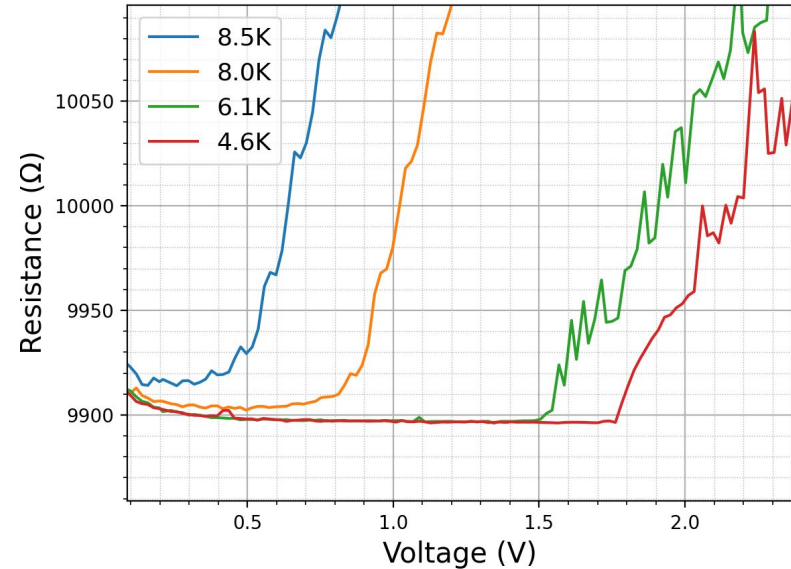
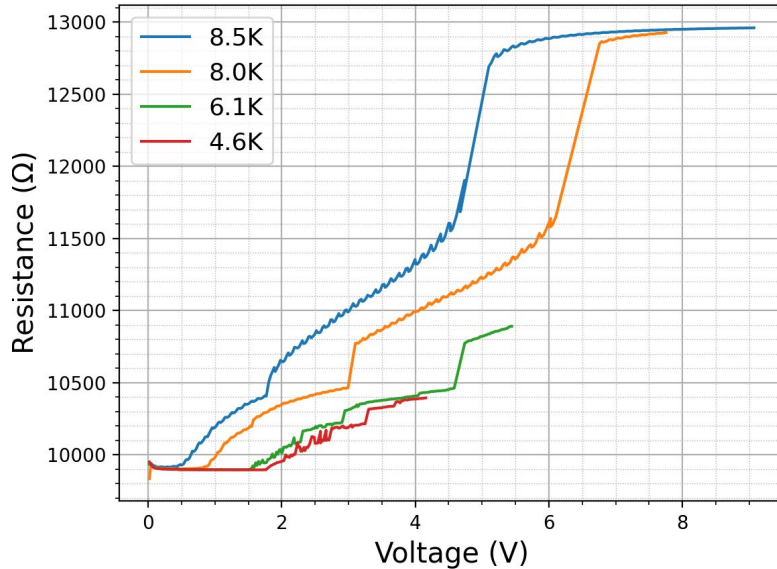
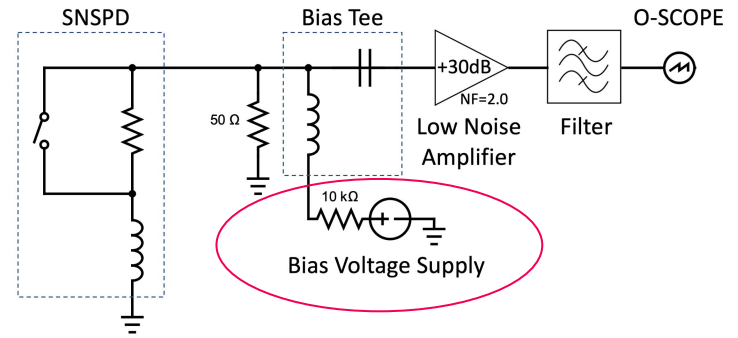
- Inductance is the tendency of an electrical conductor to oppose a change in the electric current flowing through it.
- Kinetic inductance originates from the inertial mass of mobile charge carriers
- Kinetic inductance is observed in high carrier mobility conductors (e.g. superconductors)

$$\frac{1}{2}(2m_e v^2)(n_s l A) = \frac{1}{2} L_K I^2$$

$$L_K = \left(\frac{m_e}{2n_s e^2} \right) \left(\frac{l}{A} \right)$$

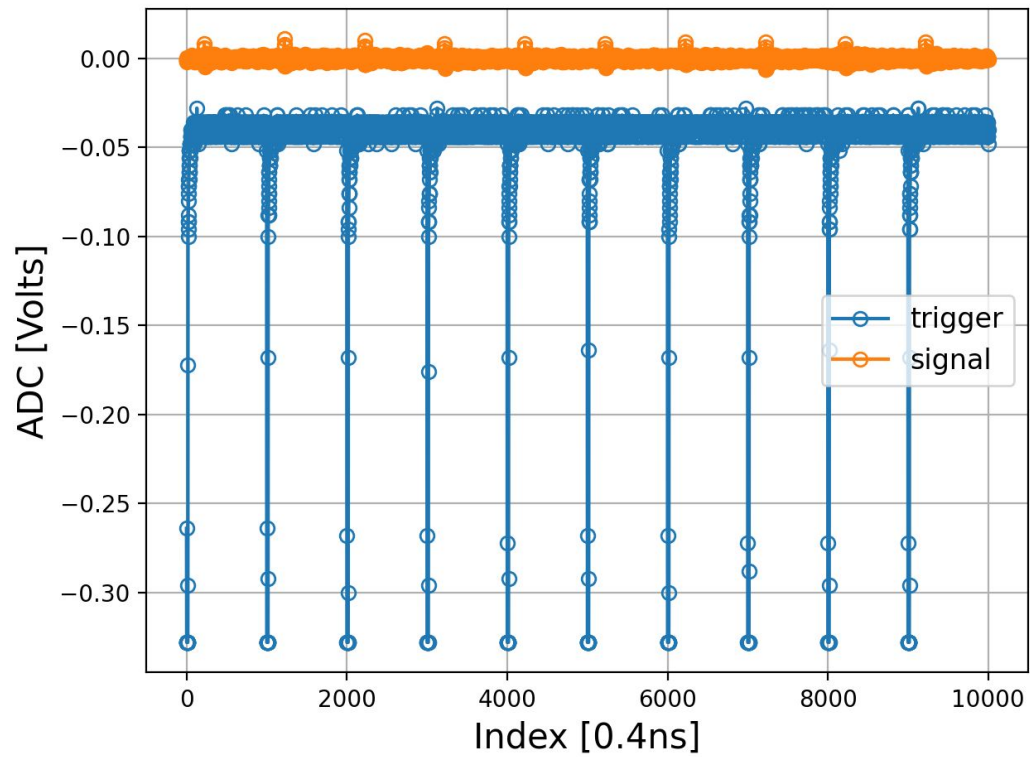
VR Curve w/ 10k Ω

- 10k Ω resistor in series with bias voltage source
- Translate bias current to voltage
- Critical Voltage @ 4.6K ~ 1.76V



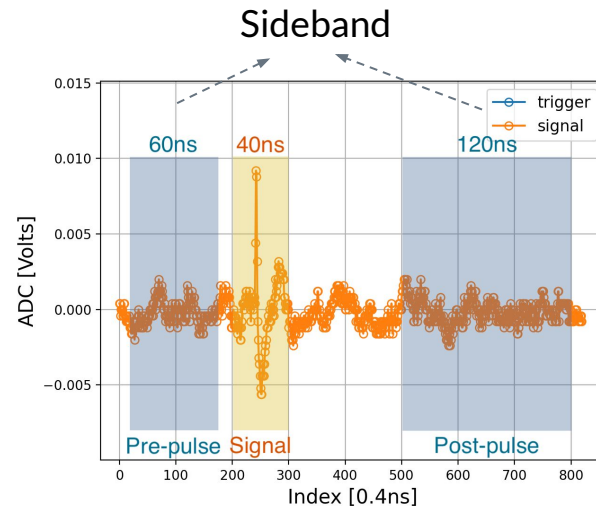
1 Oscilloscope Event

4 μ s Window \rightarrow 10 Laser Triggers

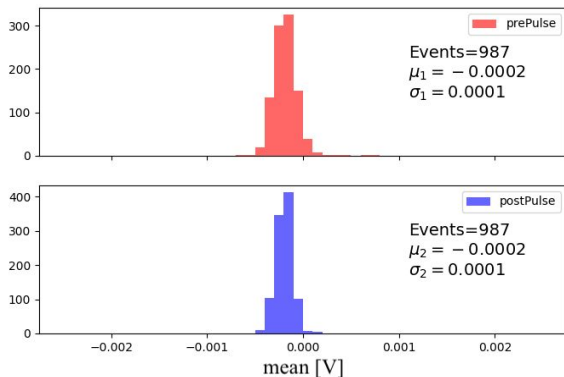


Sideband Analysis

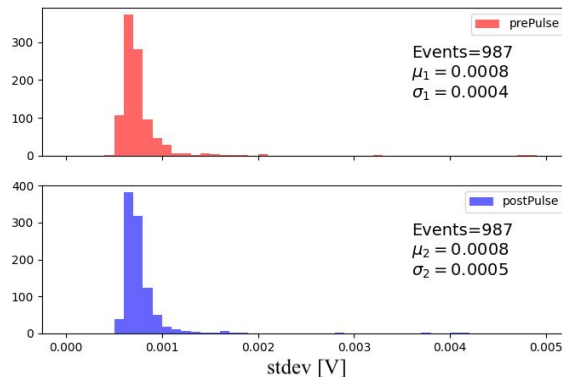
- Baseline Voltage (Mean) : $-0.2\text{mV} \pm 0.1\text{mV}$
- Average Noise (Std): $0.8\text{mV} \pm 0.4\text{mV}$
- Noise Peak-to-Peak / Random Spikes (Range): $4\text{mV} \pm 2\text{mV}$
- Sideband analysis with and without signal
 - Similar results \rightarrow Noise is uncorrelated to the signal



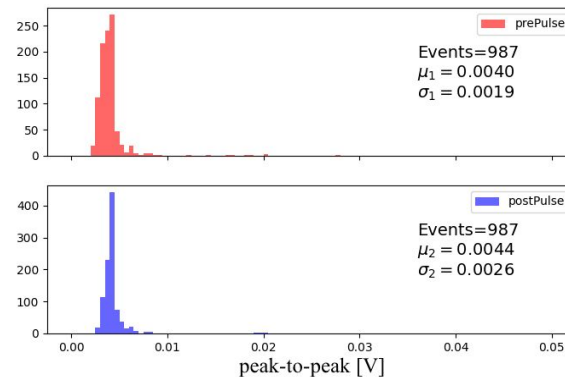
Sideband ADC Mean



Sideband ADC Standard Deviation



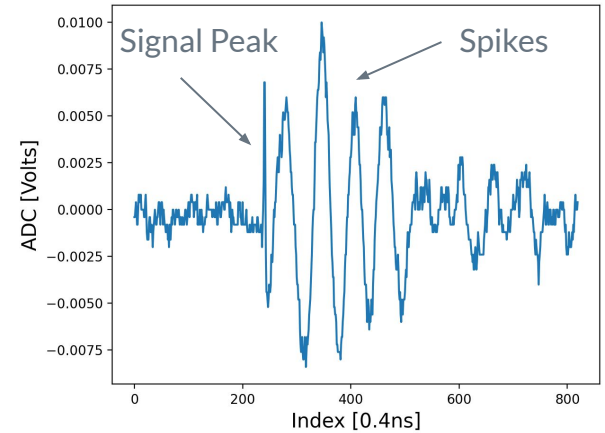
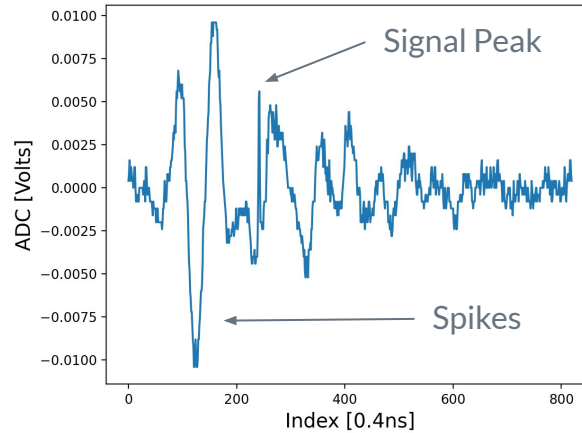
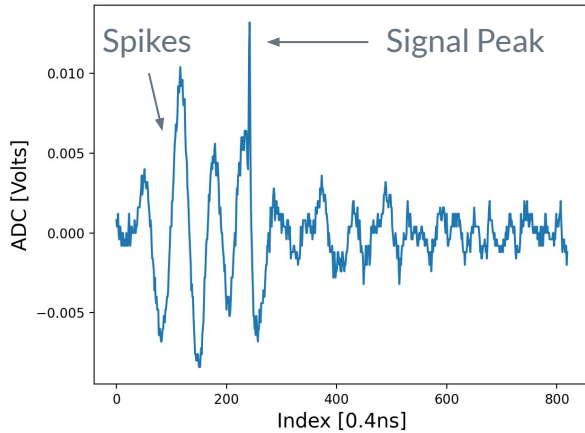
Sideband ADC Peak-to-Peak Range

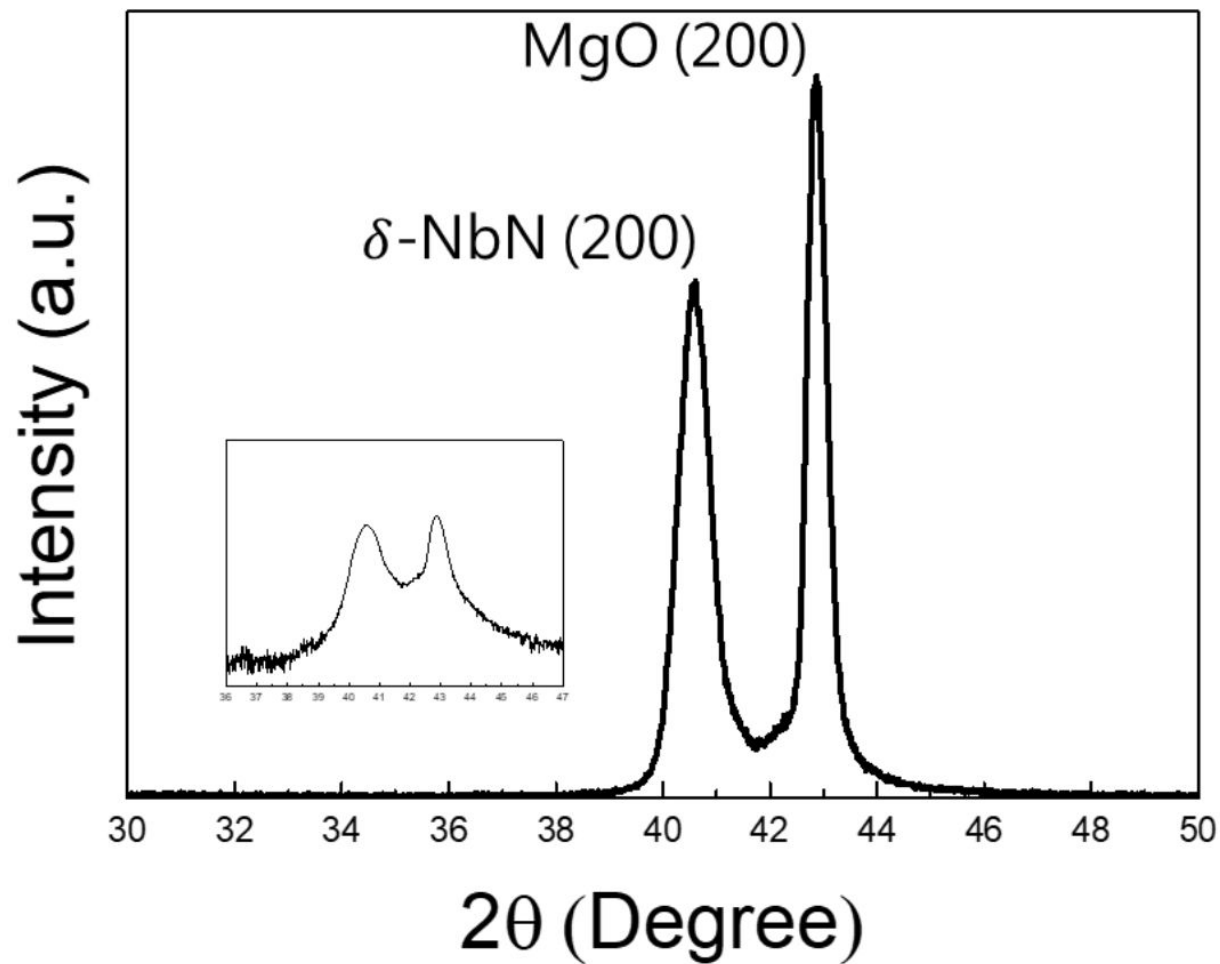


Event Pre-Selection

- Sideband Peak-to-Peak Range < 3mV
- Sideband Average Noise < 2mV

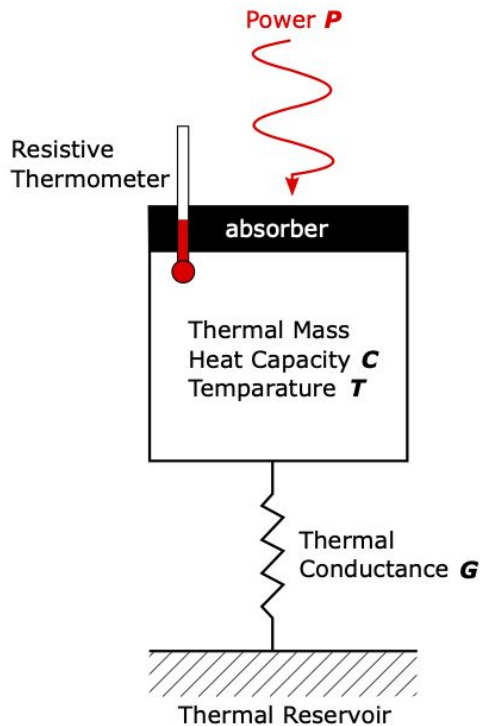
Remove laser events with large noise/spikes



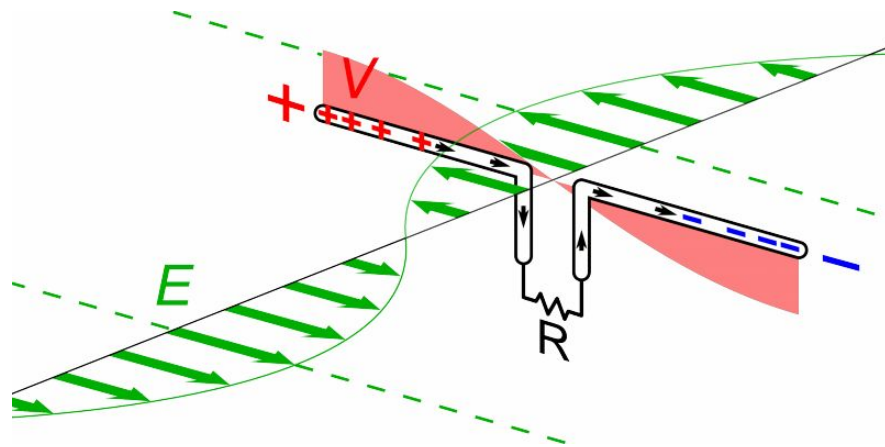


Collective Detection → Electromagnetic wave

Bolometer



Antenna



Discoveries in particle physics

Based on an original
slide by S.C.C. Ting

Facility	Original purpose, Expert Opinion	Discovery with Precision Instrument
P.S. CERN (1960)	π N interactions	
AGS BNL (1960)	π N interactions	
FNAL Batavia (1970)	Neutrino Physics	
SLAC Spear (1970)	ep, QED	
ISR CERN (1980)	pp	
PETRA DESY (1980)	top quark	
Super Kamiokande (2000)	Proton Decay	
Telescopes (2000)	SN Cosmology	

Discoveries in particle physics

Based on an original
slide by S.C.C. Ting

Facility	Original purpose, Expert Opinion	Discovery with Precision Instrument
P.S. CERN (1960)	π N interactions	Neutral Currents \rightarrow Z,W
AGS BNL (1960)	π N interactions	Two kinds of neutrinos Time reversal non-symmetry charm quark
FNAL Batavia (1970)	Neutrino Physics	bottom quark top quark
SLAC Spear (1970)	ep, QED	Partons, charm quark tau lepton
ISR CERN (1980)	pp	Increasing pp cross section
PETRA DESY (1980)	top quark	Gluon
Super Kamiokande (2000)	Proton Decay	Neutrino oscillations
Telescopes (2000)	SN Cosmology	Curvature of the universe Dark energy